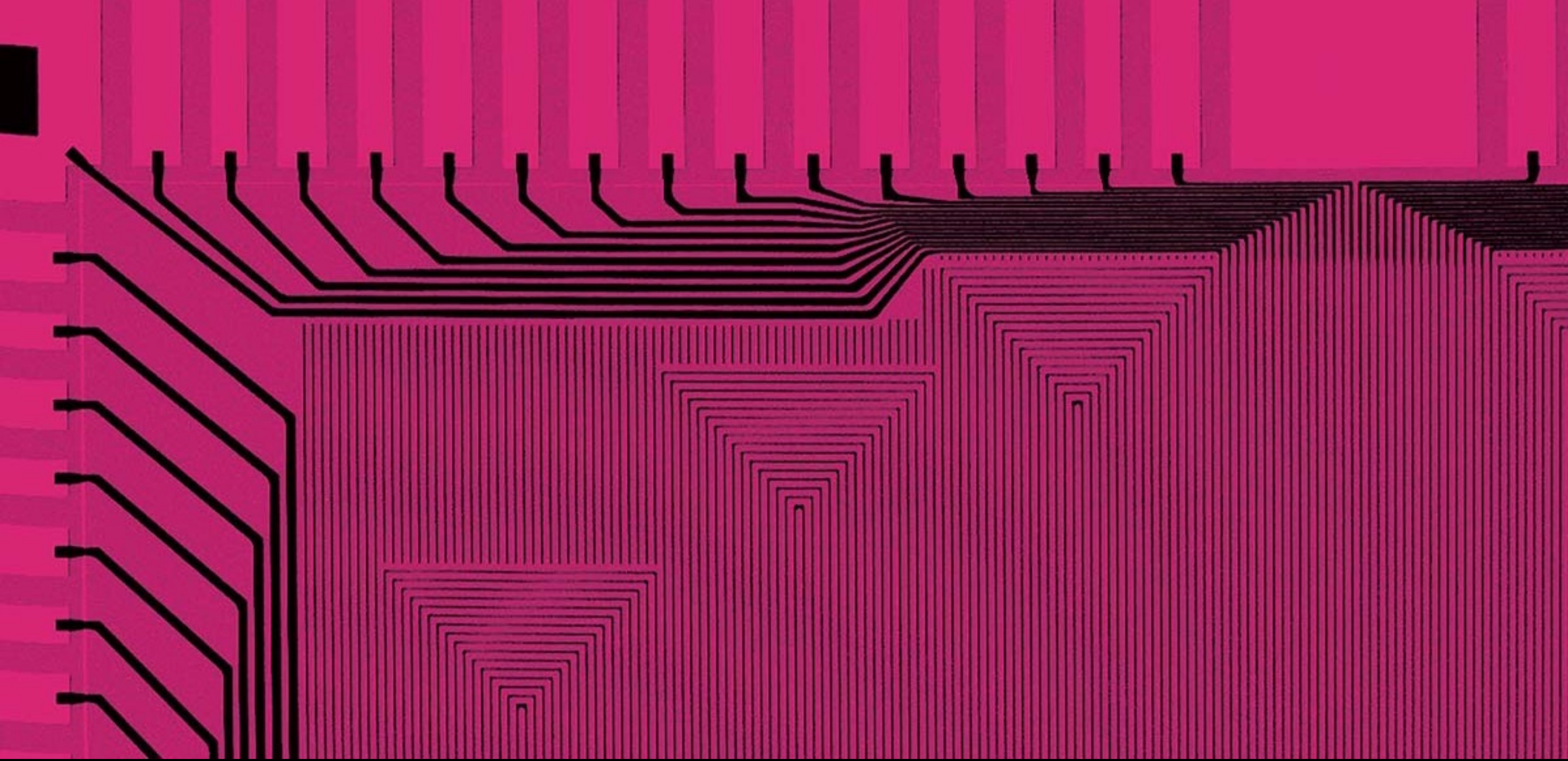

International Superconductive Electronics Conference 2019. Riverside, CA.

Development of superconducting nanowire single-photon detector arrays for current and future deep-space optical communication

Emma E. Wollman, Jason P. Allmaras, Andrew D. Beyer, Marc C. Runyan, Ryan M. Briggs, Boris Korzh, and Matthew D. Shaw

Jet Propulsion Laboratory, California Institute of Technology

Jet Propulsion Laboratory
California Institute of Technology

Why deep space optical communication?

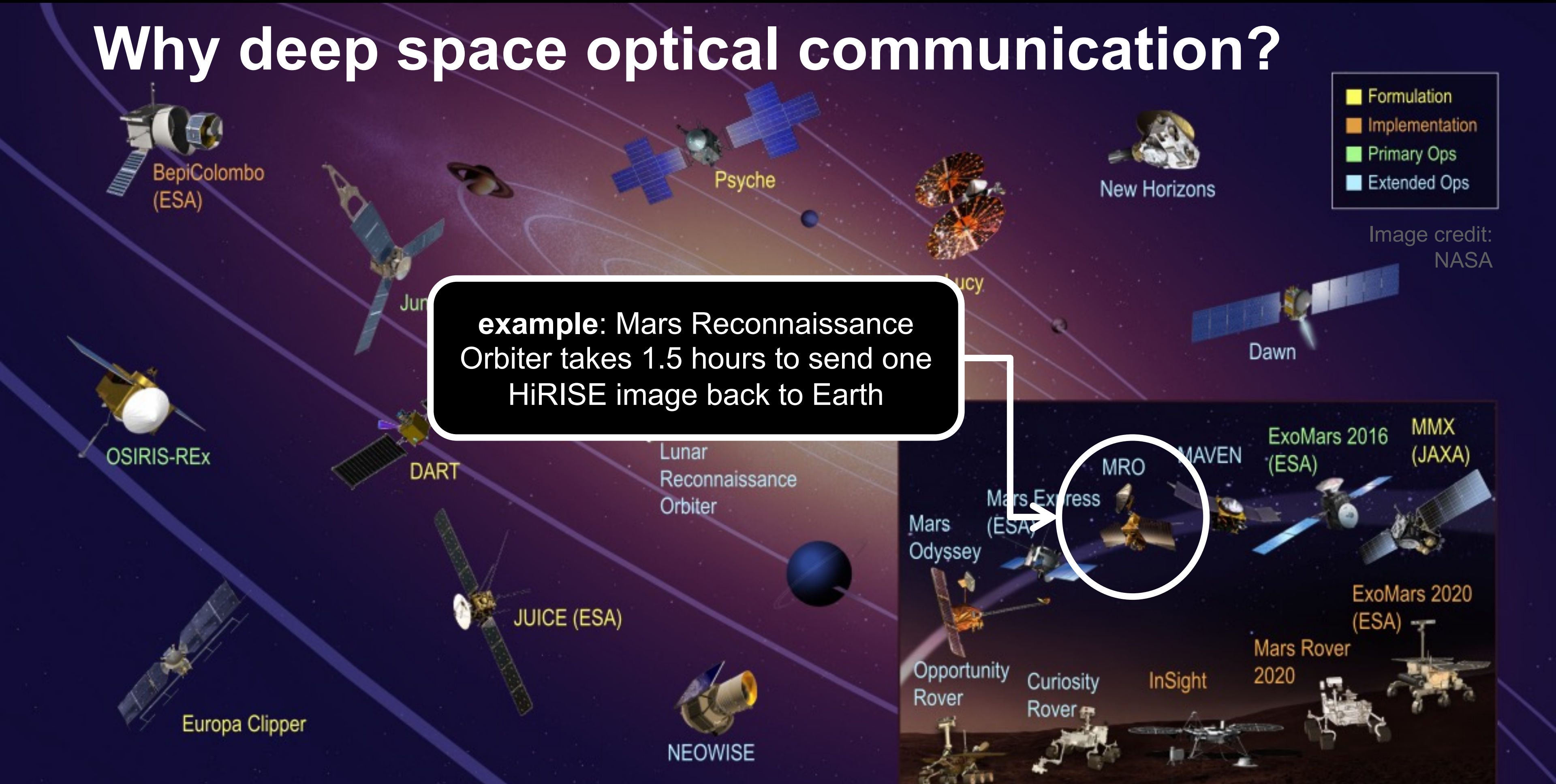

- All of NASA's interplanetary spacecraft currently communicate with Earth through the RF dishes of the Deep Space Network (DSN)
- Required data rates are expected to increase as more advanced instruments are able to capture larger volumes of data
- NASA's Space Communications and Navigation office seeks solutions to enhance and complement existing RF communication

Why deep space optical communication?

Image credit: NASA

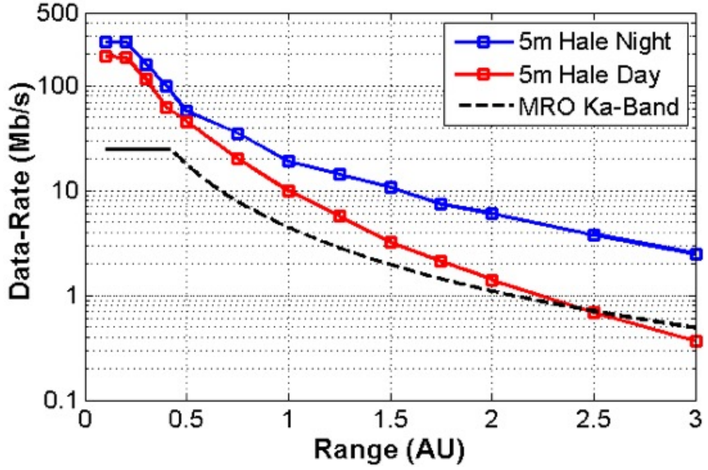

Performance using 4W average laser power w/ 22cm flight transceiver to 5m ground telescope

DSN antenna at Goldstone, CA

- Optical communication promises **10-100x** more data than Ka-band RF links for equivalent mass and power on the spacecraft
- Will require a network of large (~10m) telescopes
- Currently, deep space optical communication missions are limited to technology demonstration missions with more moderate data rate increases

Lunar Laser Communication Demo (2013-2014)

- Bidirectional laser communication demo from LADEE Spacecraft in lunar orbit (400,000 km) at 1550 nm
- First demonstration of laser communication beyond earth orbit
- Uplink rates 10-20 Mbps, Downlink rates 39-622 Mbps
- Managed by GSFC, Transmit payload and primary ground terminal at White Sands, NM implemented by MIT-LL
- Secondary ground terminal at Table Mountain, CA implemented by JPL
- Both ground terminals used SNSPD arrays

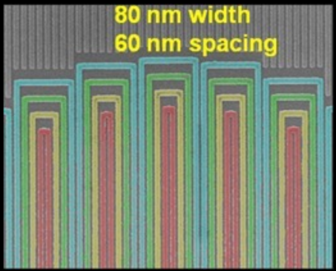

4-channel MIT-LL NbN SNSPD array

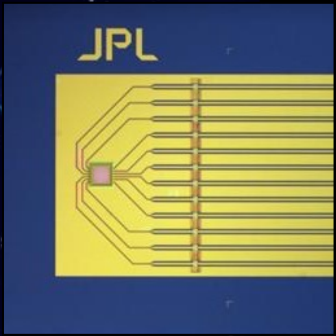

16-channel JPL WSi SNSPD array

Image credit: NASA

Deep space optical communication (DSOC) project

- DSOC is a **technology demonstration mission** planned to launch on board NASA's Psyche mission in 2022
- Psyche's trajectory takes it past Mars to the asteroid belt, where it will study the metal asteroid **16 Psyche**
- The maximum Earth-spacecraft distance will be **2.77 AU**

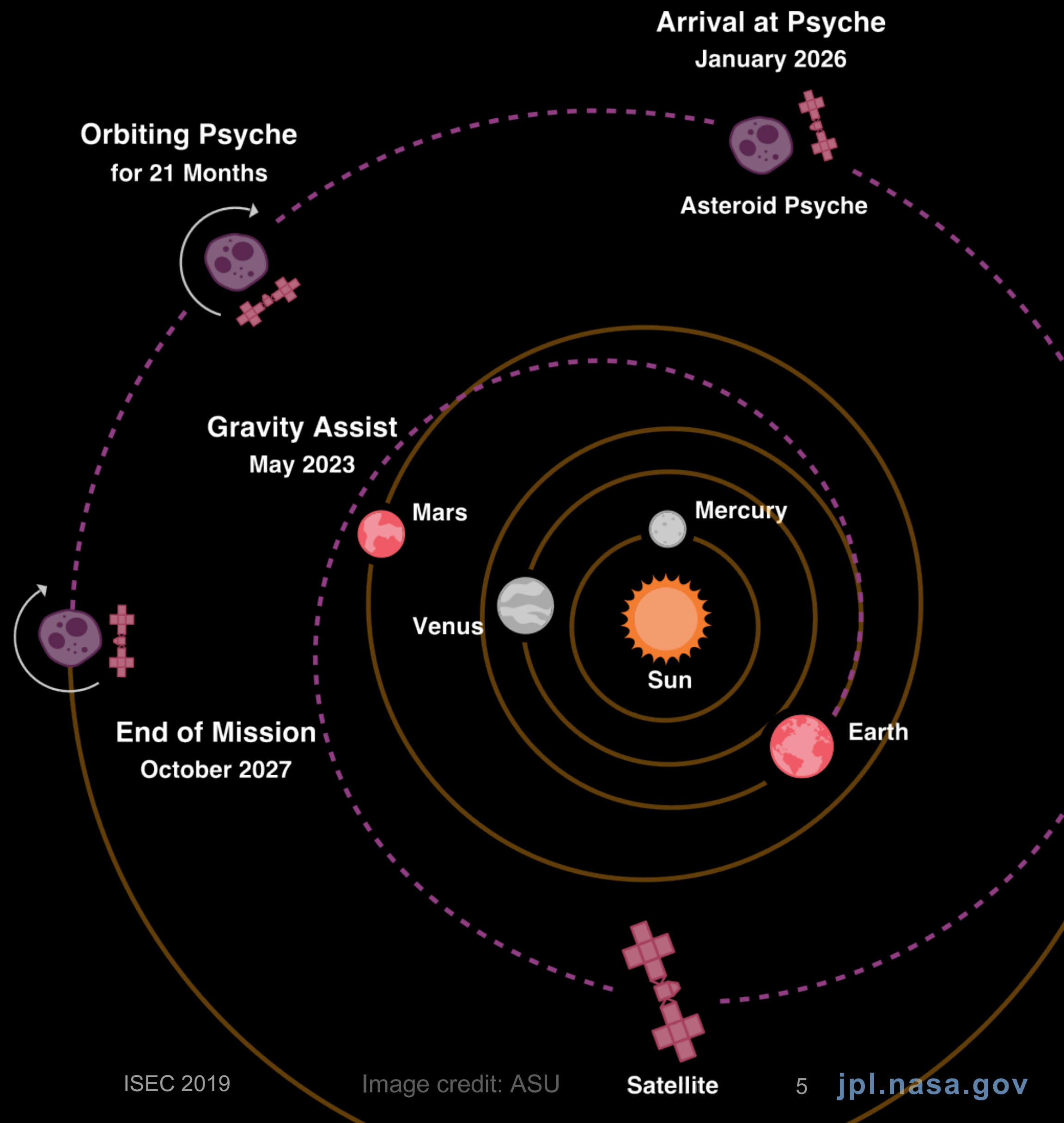

Image credit: ASU

Pre-Decisional Information –
For Planning and Discussion Purposes Only

Deep Space Optical Communications (DSOC)

OBJECTIVES: Demonstrating optical communications from deep space (0.1 – 2.7 AU) at rates up to 267 Mbps to validate:

- Link acquisition laser pointing control
- High photon efficiency signaling

Psyche spacecraft

1550 nm downlink

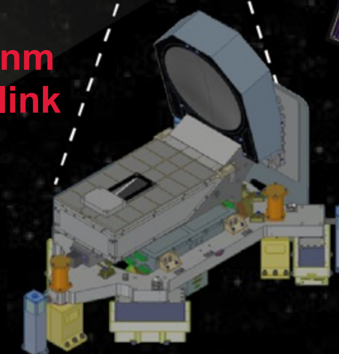

Optical Platform Assembly
22 cm mirror
4 W laser power

1064 nm uplink

Ground Laser Transmitter
Table Mtn, CA
1 m OCTL telescope
5 kW laser power

Ground Laser Receiver
Palomar Mtn, CA
5 m Hale telescope

Deep space challenges

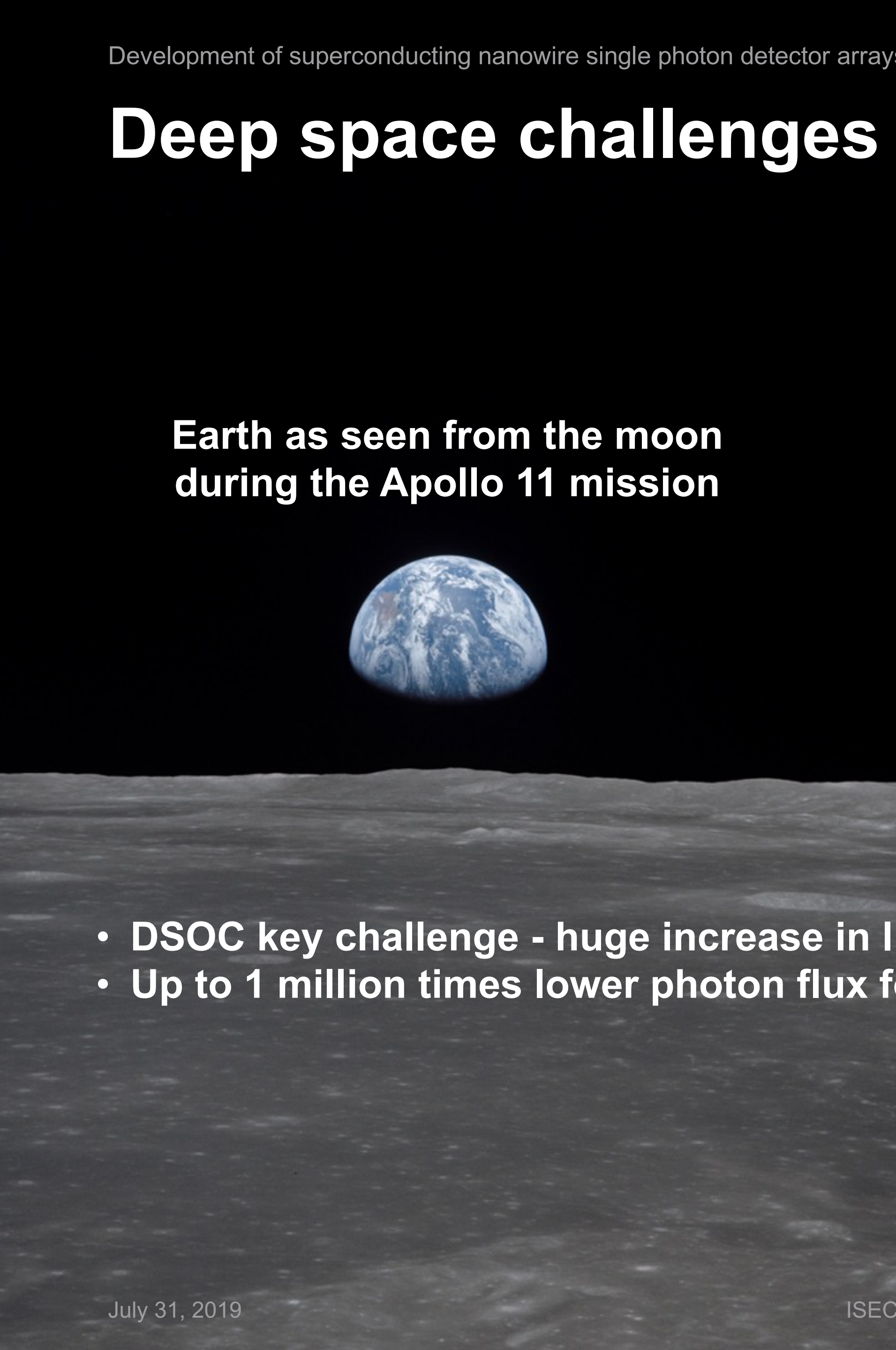

Earth as seen from the moon during the Apollo 11 mission

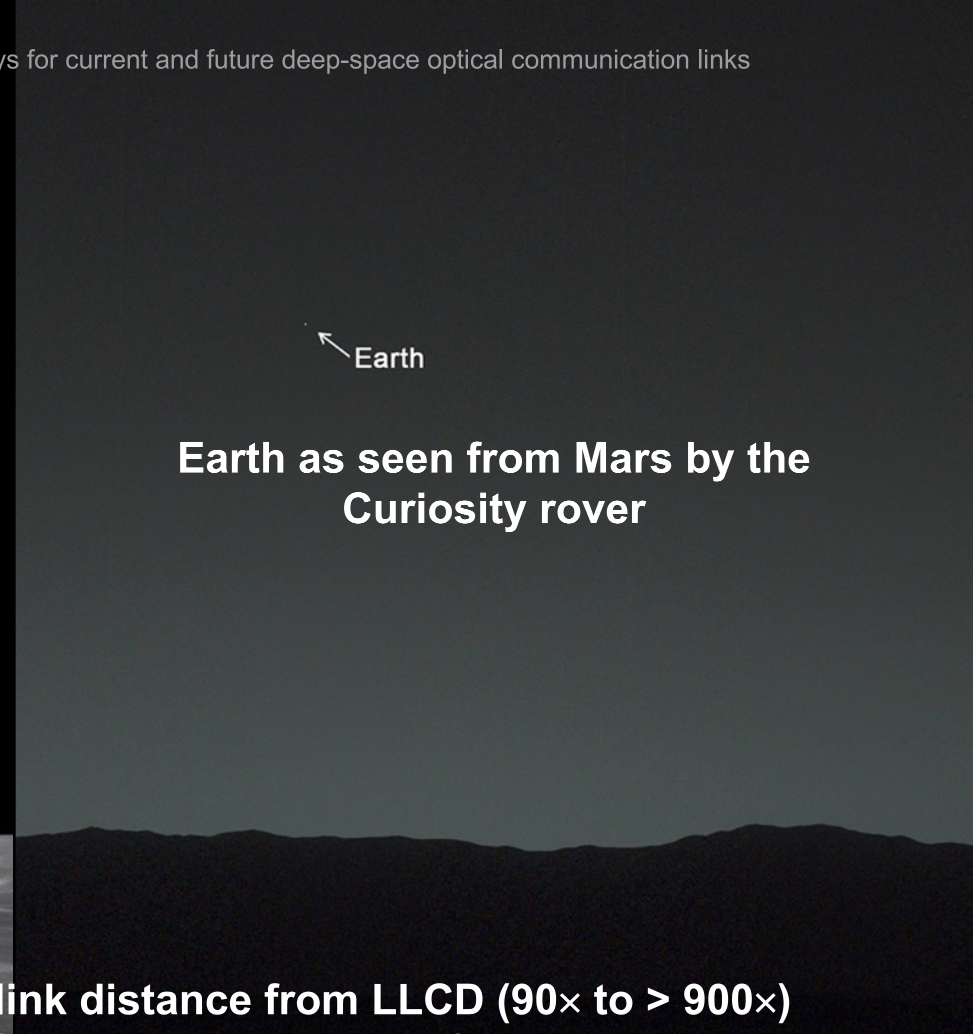

Earth as seen from Mars by the Curiosity rover

- **DSOC key challenge - huge increase in link distance from LLCD (90× to > 900×)**
- **Up to 1 million times lower photon flux for same design as LLCD!**

Deep space challenges

Earth as seen from the moon during the Apollo 11 mission

Earth as seen from Mars by the Curiosity rover

- **DSOC key challenge - huge increase in link distance from LLCD (90× to > 900×)**
- **Up to 1 million times lower photon flux for same design as LLCD!**
  - Increase transmitter laser power (4 W vs. LLCD 0.5 W)
  - Increase ground receiver collection area (5 m vs. ~ 1 m)
  - Decrease beam divergence (8 μrad vs. LLCD 16 μrad): **introduces pointing challenge**
  - Increase ground detector sensitivity

Deep space challenges

Maximum spot size
(spacecraft / Earth distance = 2.77 AU)

- **DSOC key challenge - huge increase in link distance from LLCD (90× to > 900×)**
- **Up to 1 million times lower photon flux for same design as LLCD!**
  - Increase transmitter laser power (4 W vs. LLCD 0.5 W)
  - Increase ground receiver collection area (5 m vs. ~ 1 m)
  - Decrease beam divergence (8 μrad vs. LLCD 16 μrad): **<u>introduces pointing challenge</u>**
  - Increase ground detector sensitivity

Increasing receiver sensitivity: High photon efficiency signaling

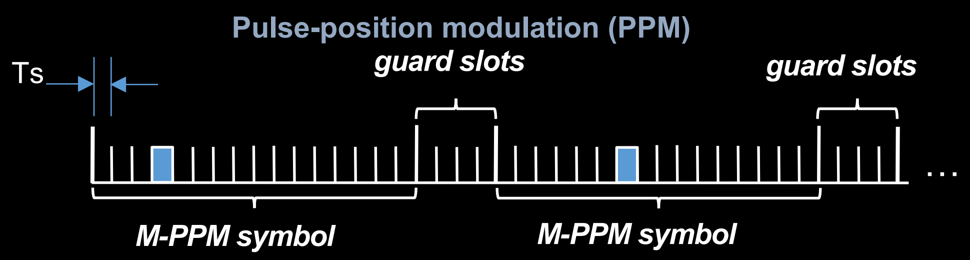

Fading causes burst outages

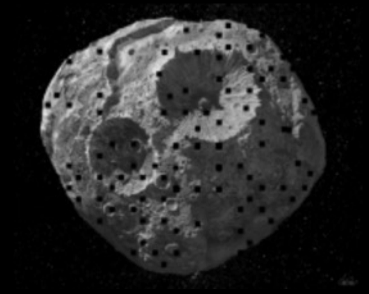

Decoder corrects more errors spread across codewords by interleaver

- **High peak-to-average power ratio (20:1 to 160:1)**
- **Pulse-position-modulation (PPM)** with variable orders (M = 16 - 128; Ts = 0.5 - 8 ns)
- **Near-channel-capacity forward error correction**: serially concatenated convolutionally coded PPM (SC-PPM) with variable code rates (1/3, 1/2, 2/3)
- **Interleaving for fading mitigation**: convolutional channel interleaver
  - Distributes deep fades across codewords to allow decoder to work (~3 dB recovered)
  - Designed with 2.7 sec depth for all data rates (based on pointing jitter estimates)
- **Lower data rates for far ranges** with variable symbol repeat factors and slot-widths (0.5 - 8 ns) – enable multitude of rates from < 1 MHz to > 100 MHz

Photon-counting PPM reception

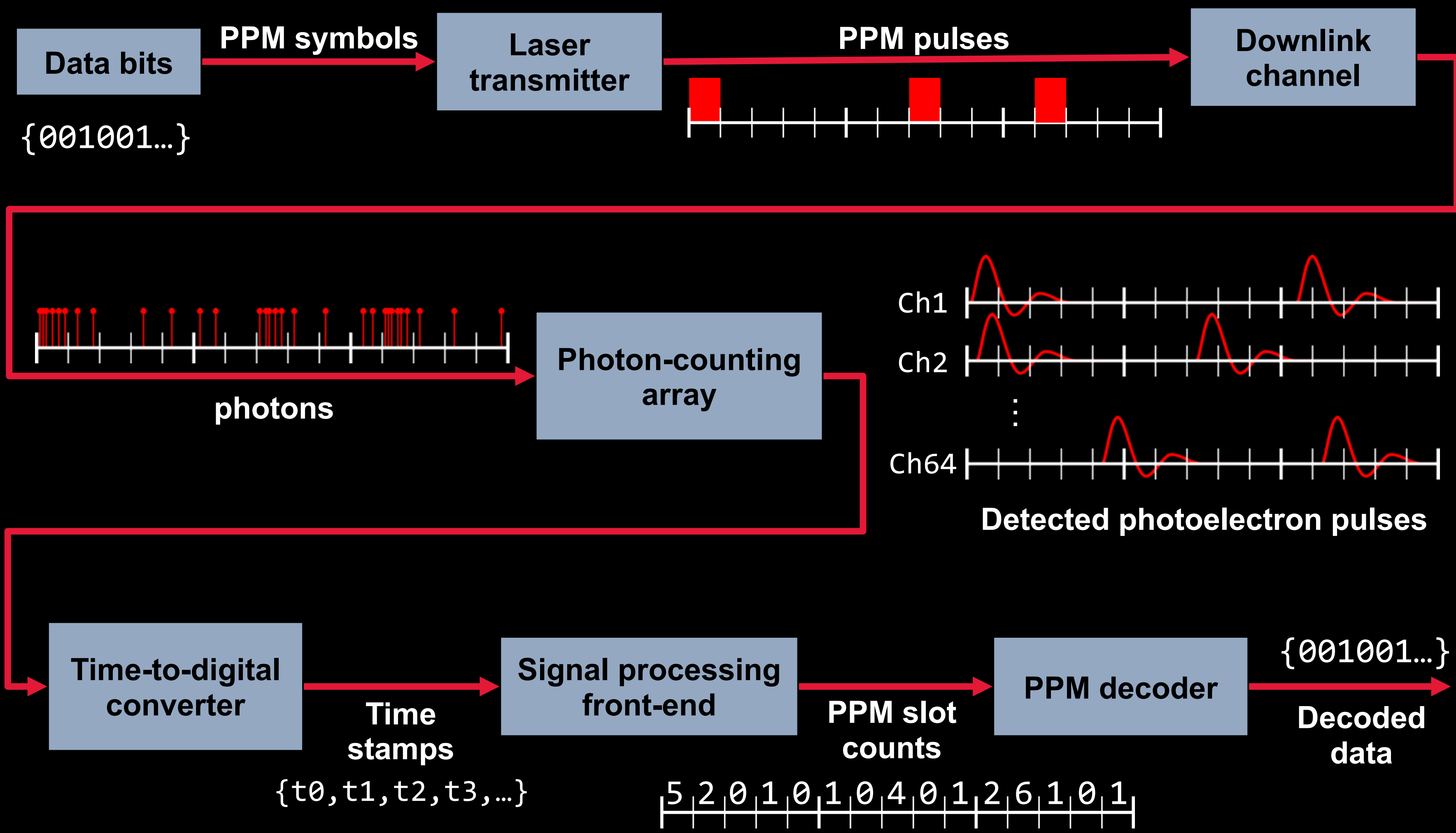

Increasing receiver sensitivity: collection area

Accommodation at Palomar Observatory

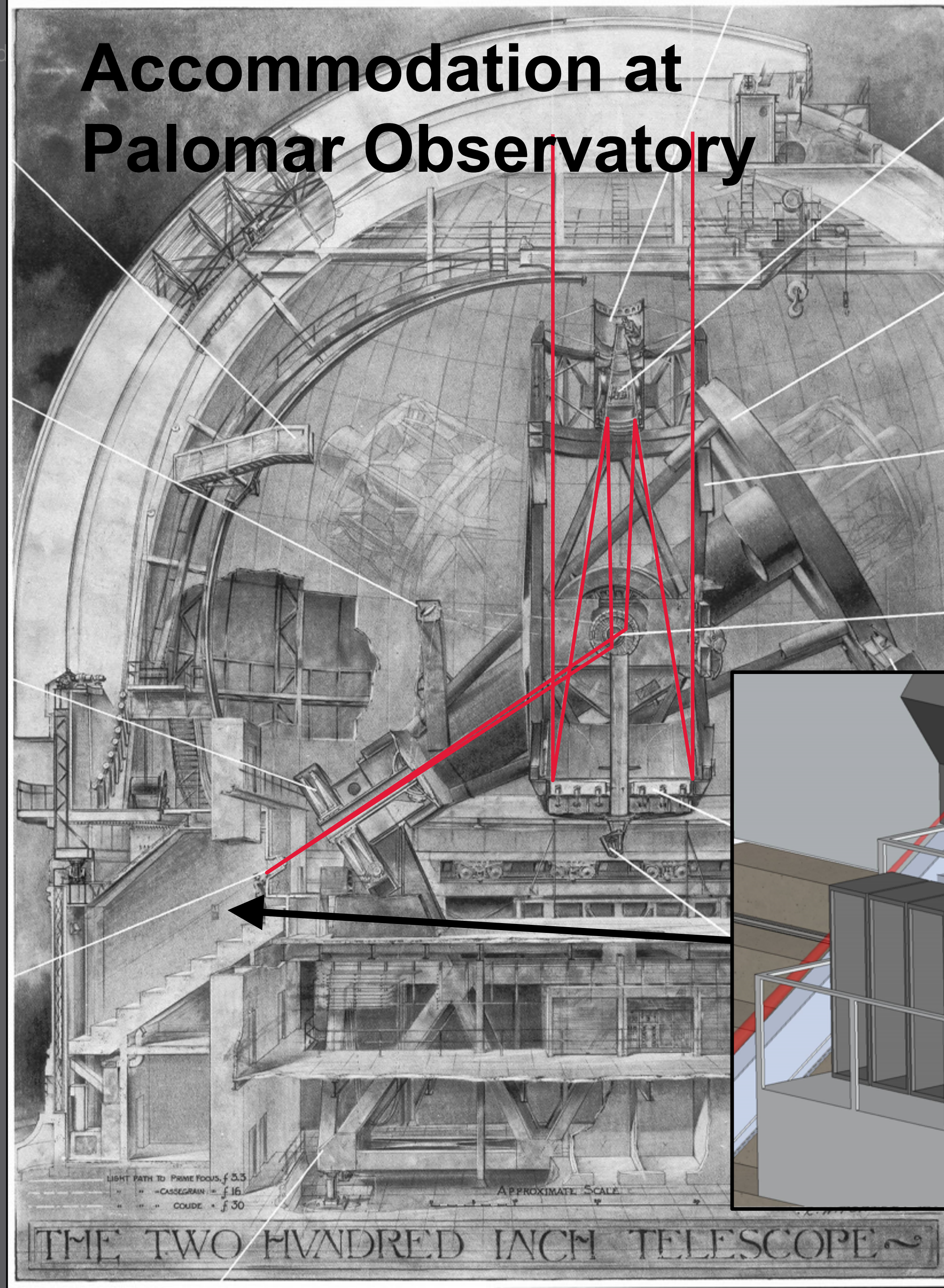

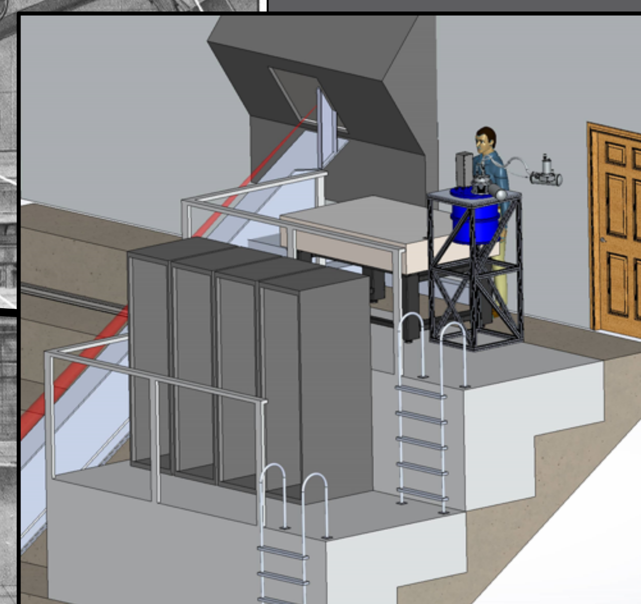

Desired detector capabilities

Clarify SDE conditions

Metric	Ideal detector	Best SNSPD performance (specialized devices)	Target detector system performance
Active area	Arbitrarily large	1 mm	90-250 um spot sizes (1/e^2 diam)
Angle of acceptance	Arbitrarily large	Typically fiber-coupled (NA < 0.15)	Beam NA of up to 0.32
Detection efficiency	100%	> 95%	67.5% (75%
Dark count rate	0	10^-4 cps	128 kcps
Blocking loss	None	1 Gcps (3dB saturation)	700 Mcps (3dB saturation)
Timing jitter	None	< 3 ps (FWHM)	< 100 ps (FWHM)

Ground receiver array design

Typical fiber-coupled single-pixel active area

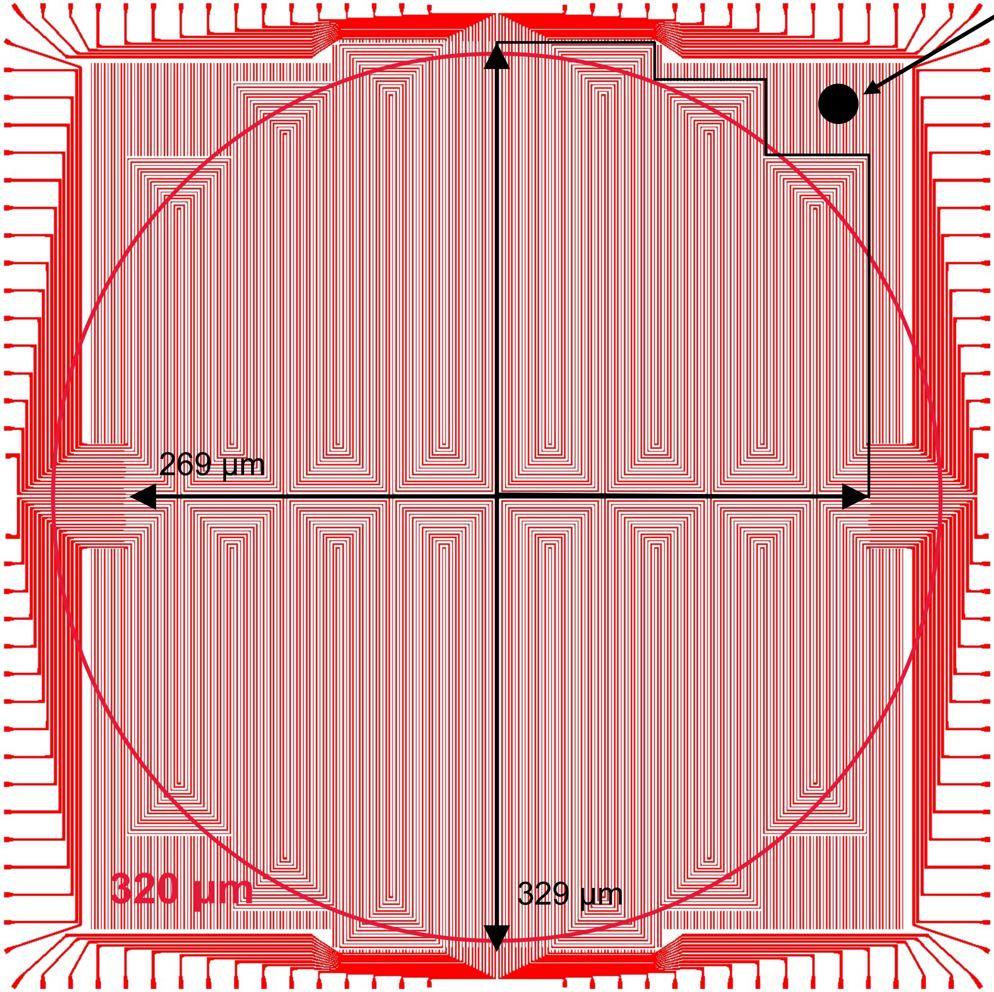

CAD Design of SNSPD focal plane array

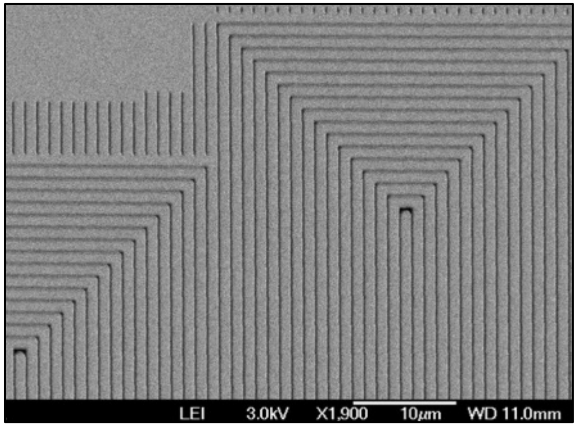

SEM of co-wound wires

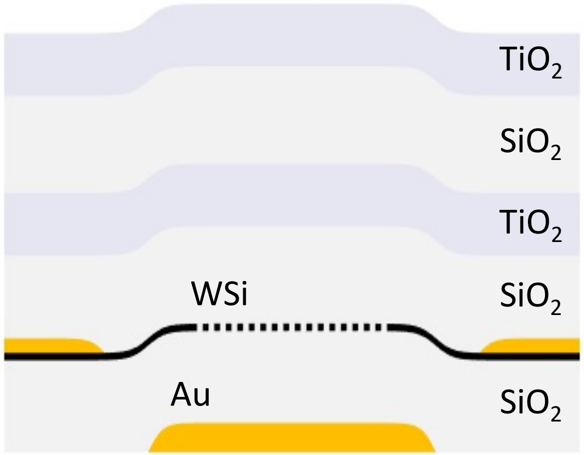

Cross-section of optical stack

160 nm WSi nanowires on 1200 nm pitch; each wire ~1 mm in length (~7000 squares)

Fabrication and yield: room temperature screening

- A. Beyer & R. Briggs fabricated devices on 3 wafers in JPL's Microdevices Laboratory. Each wafer has 44 dies.
- Room temperature screening for connected pixels and reflectance to identify most promising devices

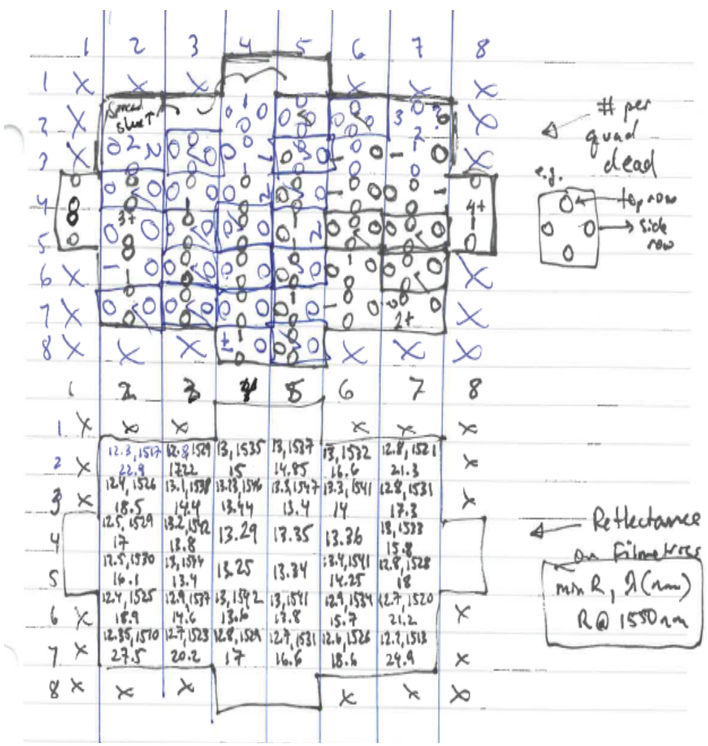

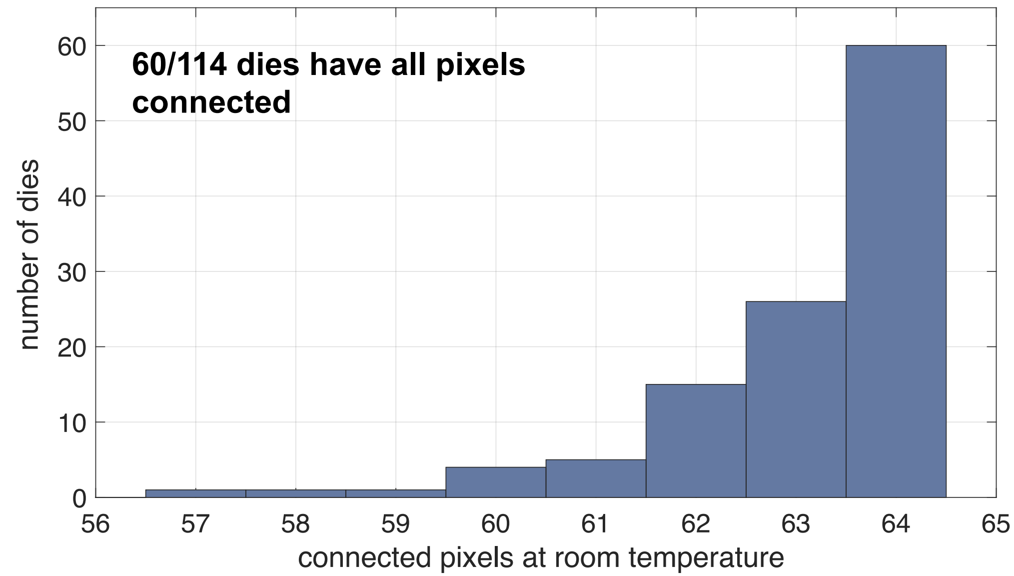

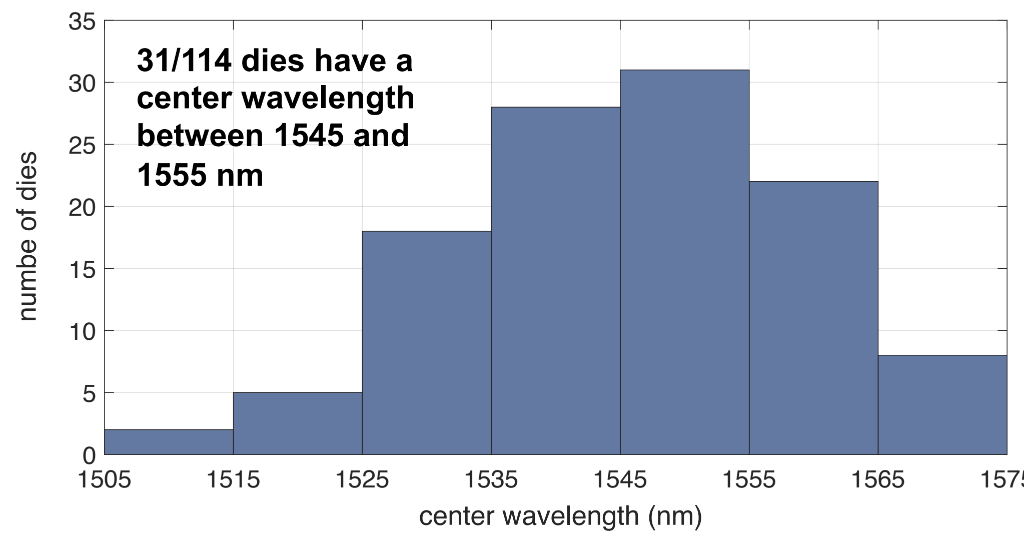

Fabrication and yield: cryogenic screening

- Promising devices from the three wafers were packaged and screened at low temperatures for efficiency, jitter, and dead time.
- All arrays with 63 or 64 saturated channels are measured to have the same detection efficiency within the +/- 2% uncertainty of the measurements.
- All arrays with 63 or 64 channels meet the detector requirements

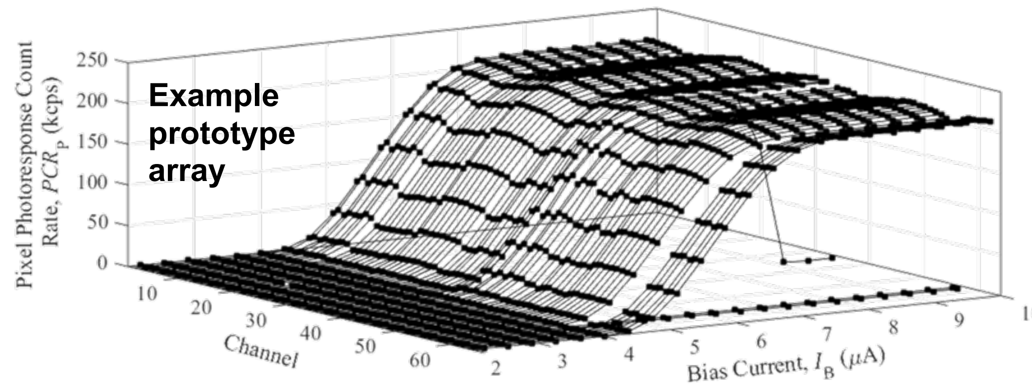

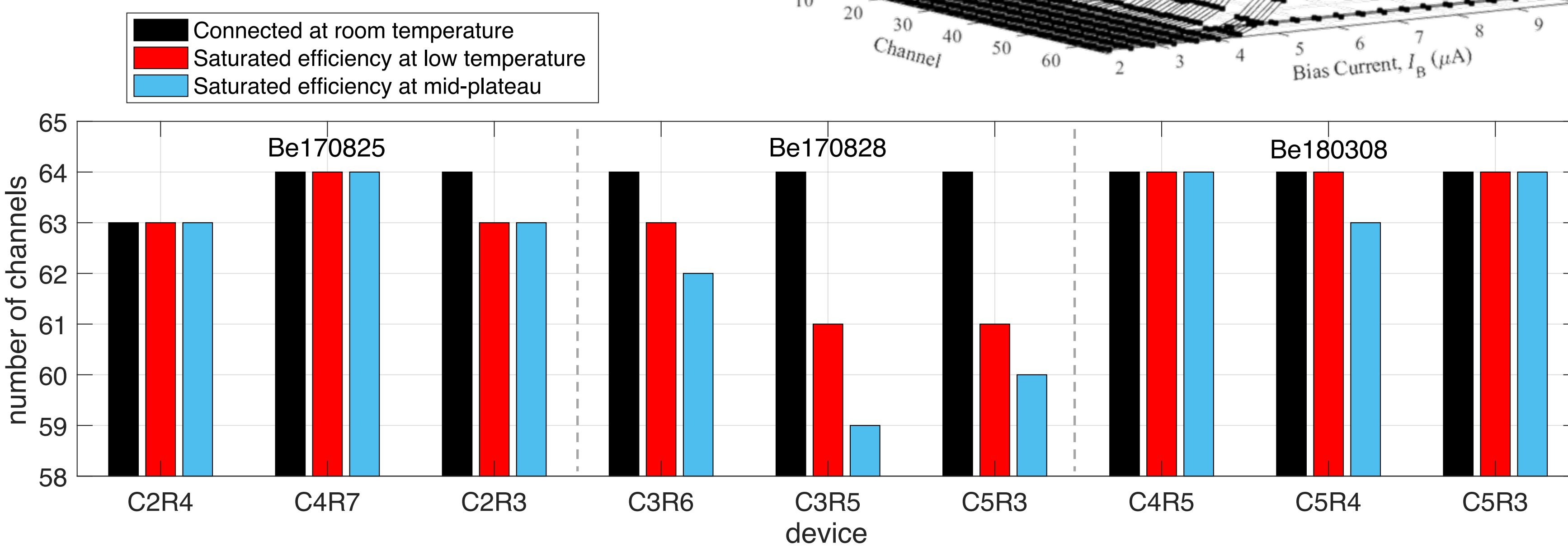

Ground detector / receiver system

Each nanowire sensor element has its own dedicated readout channel

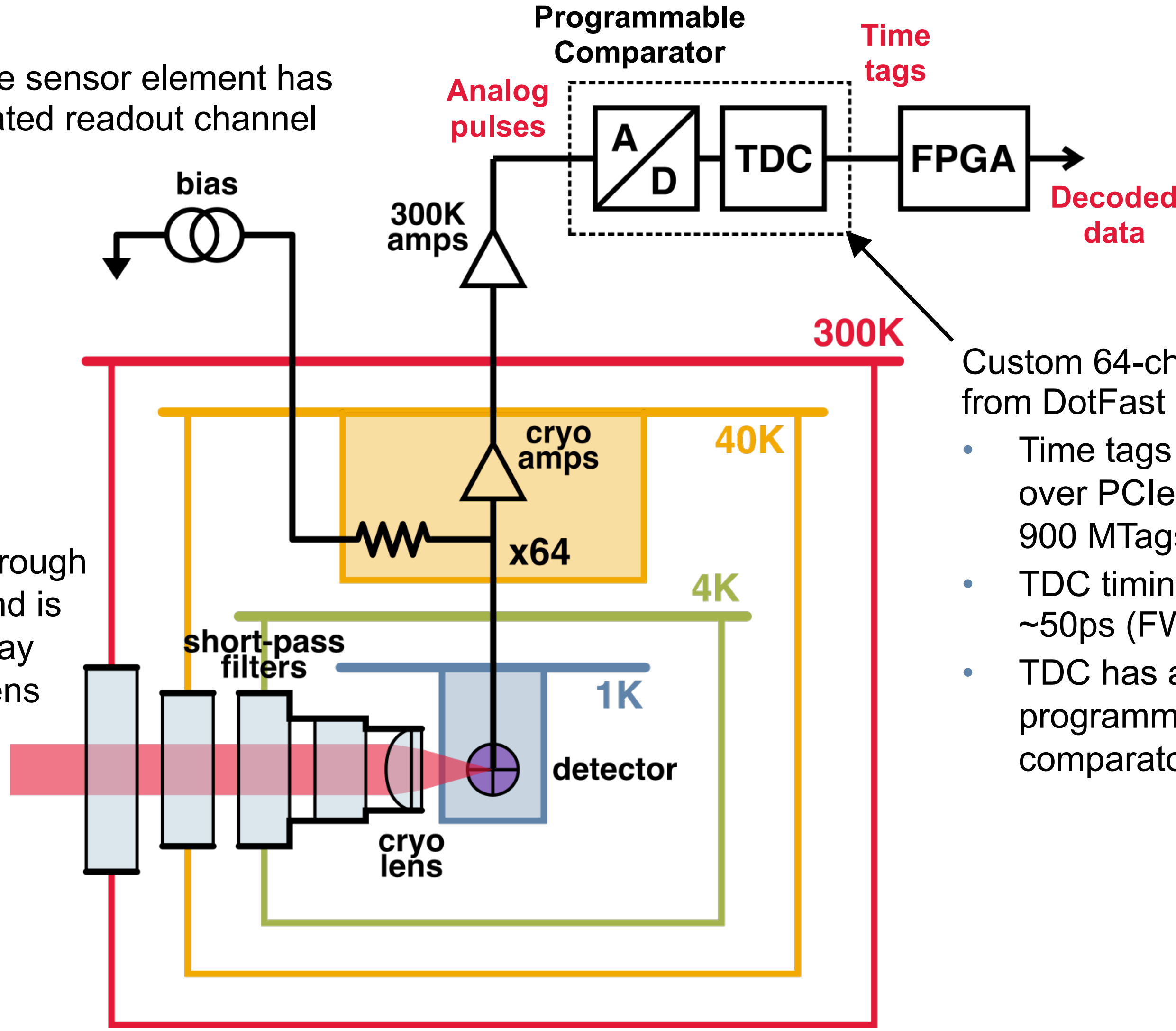

Light entering the cryostat passes through cryogenic filters and is focused on the array with a cryogenic lens

Custom 64-channel TDC from DotFast Consulting

- Time tags are streamed over PCIe at rates up to 900 MTags/s
- TDC timing resolution ~50ps (FWHM)
- TDC has a 64-channel programmable comparator front-end

Side note: 64-channel readout for imaging arrays

1032-pixel array fabricated at NIST

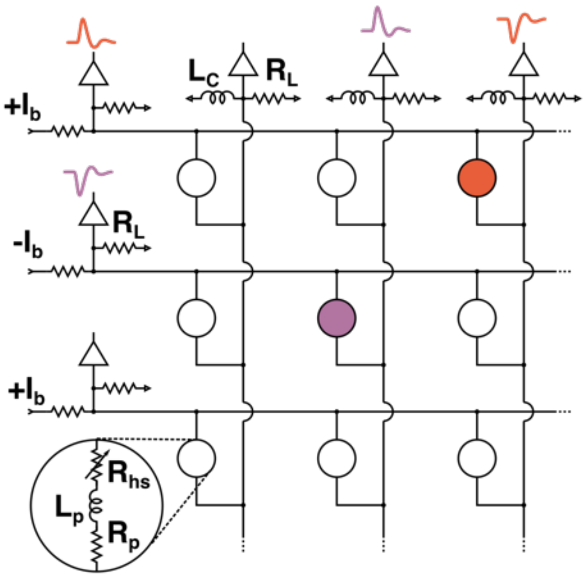

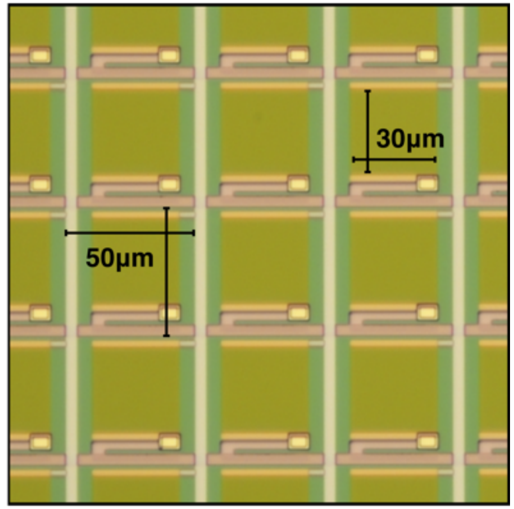

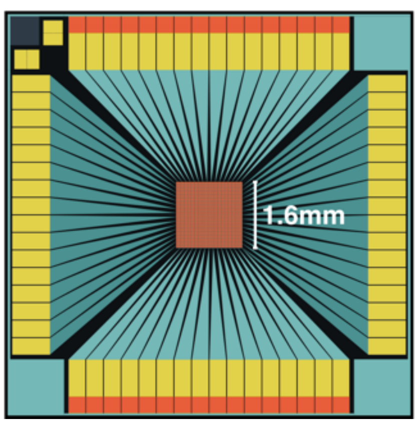

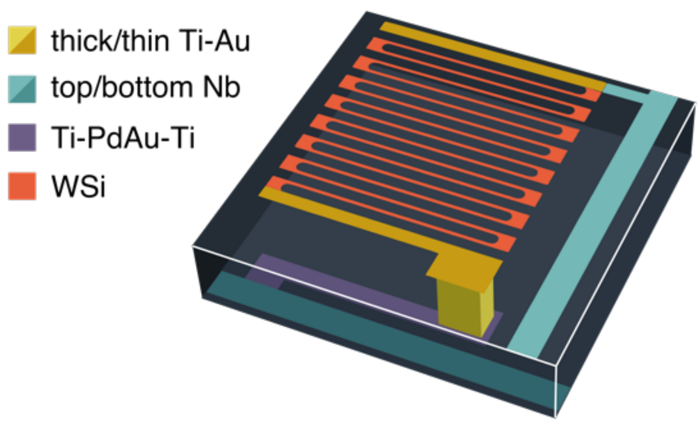

System detection efficiency

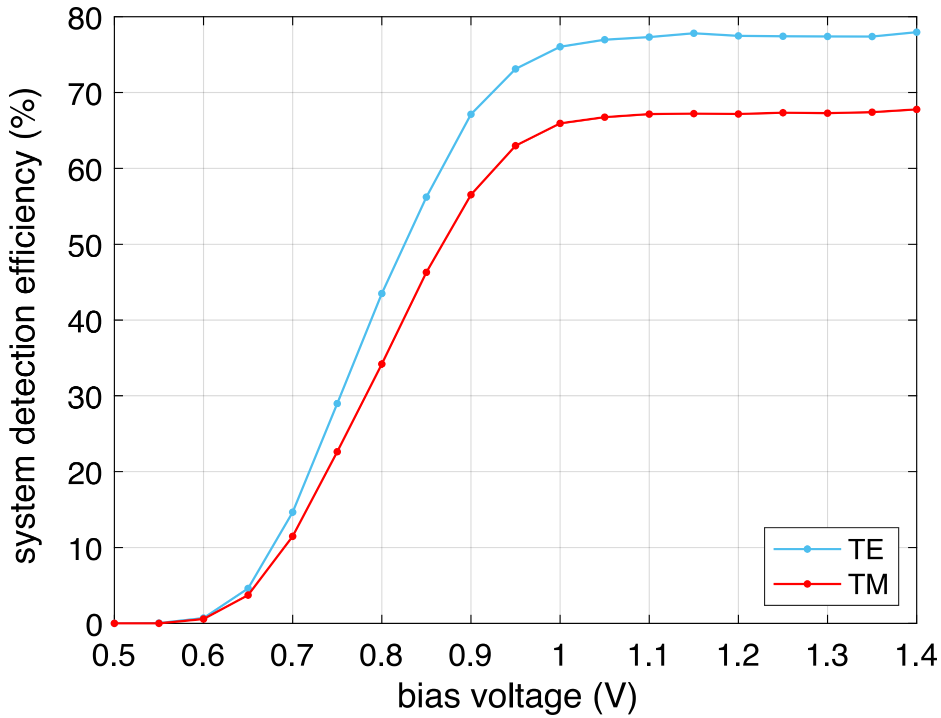

- 78% System Detection Efficiency in TE Polarization, 68% in TM. (+/- 5% uncertainty)
  - Defined as percent of photons incident on the cryostat window that are registered by the TDC.
- Measured at low flux (~100 kcps) with lens outside the cryostat (f/4 beam)
- Measured with ~230 µm diameter spot in center of array
- Prototype array has 62 out of 64 pixels working – screening arrays to find 64 perfect wires

Array spatial model

- Layout of co-wound nanowires leads to non-uniform absorption across the array

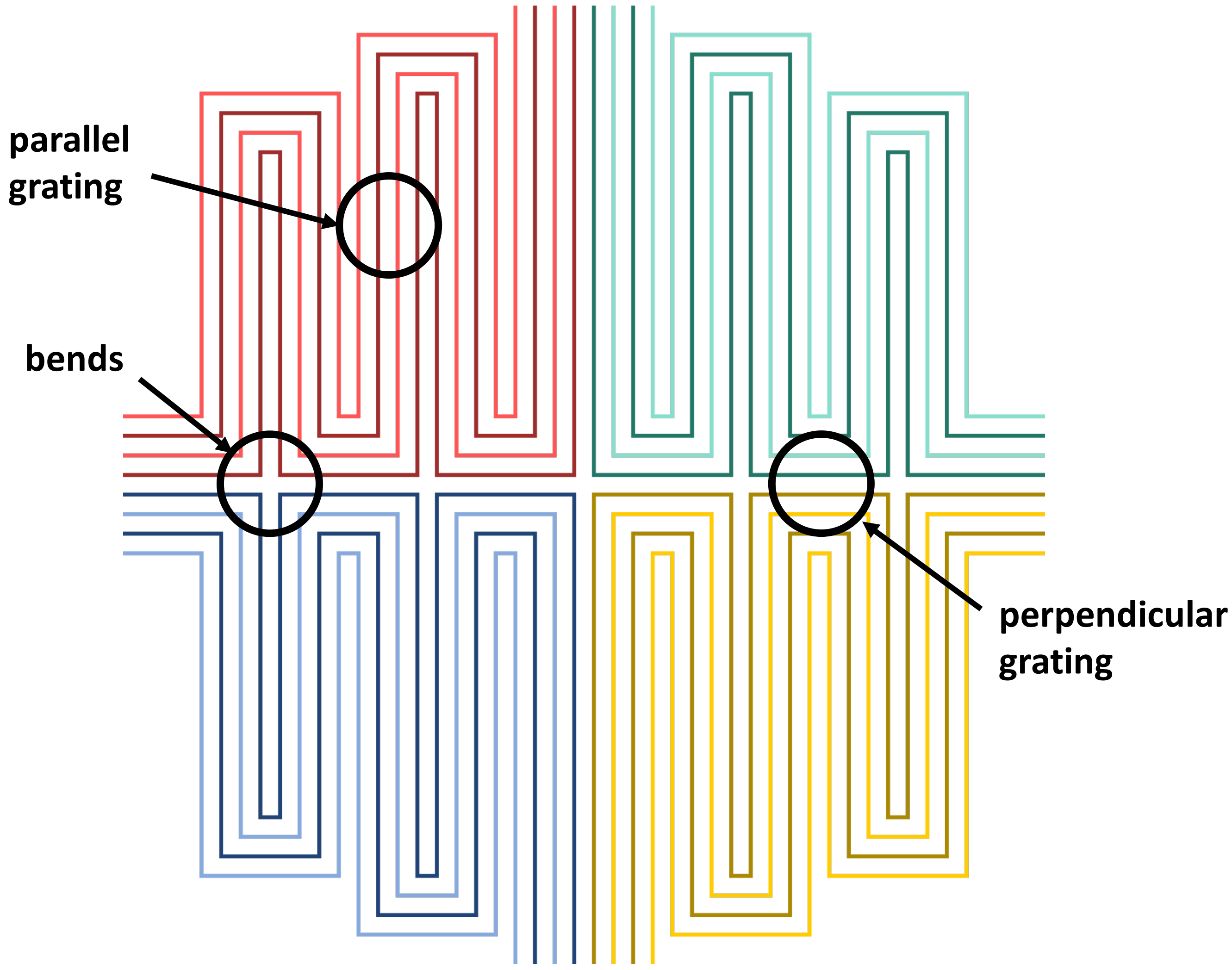

Array spatial model

Model fit to channel efficiency to determine $\eta_{||}$ and $\eta_{\perp}$

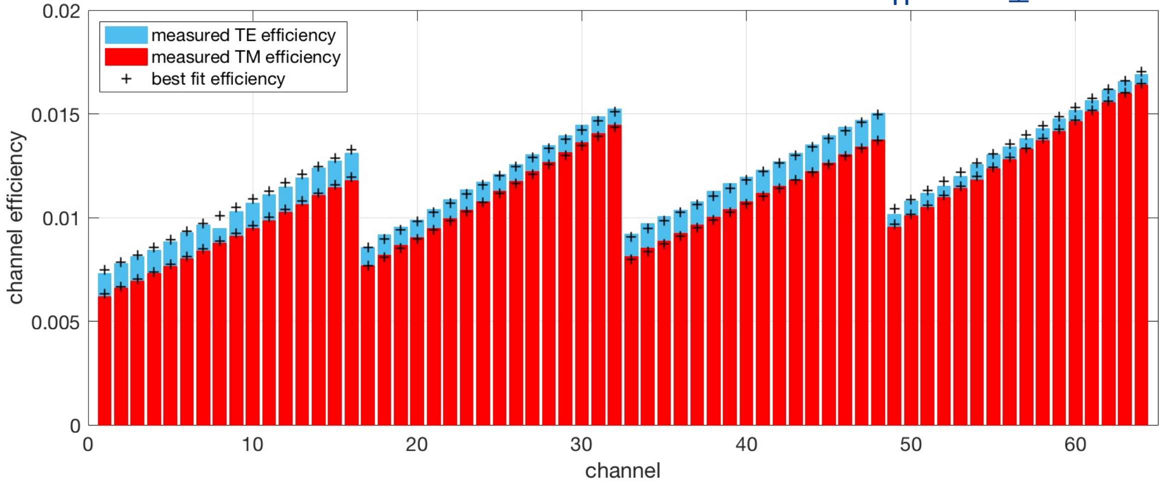

Measured spatial efficiency map

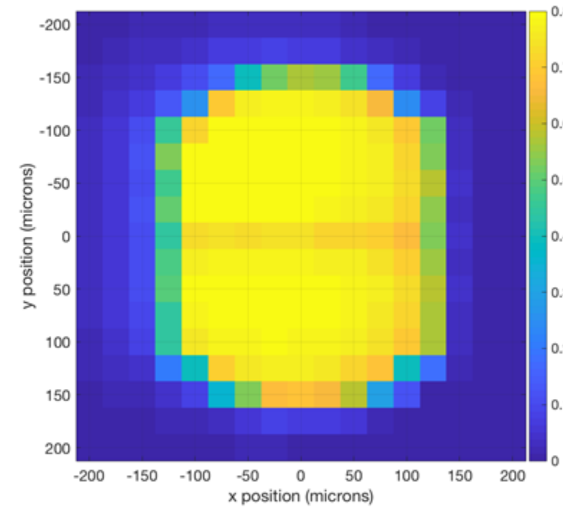

Modeled spatial efficiency map

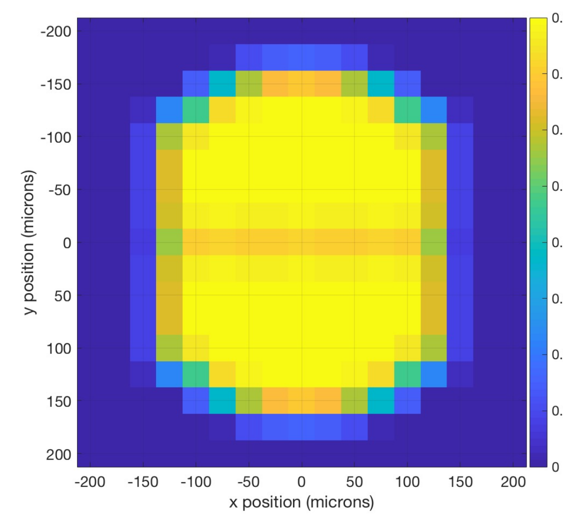

- We can model the absorption into each channel (above) as well as the overall array efficiency for an arbitrary intensity distribution.
- Example: map of efficiency vs. spot position for a 50-micron diameter Gaussian spot.
- Data is in good agreement with predictions of the model.

Efficiency as a function of spot size

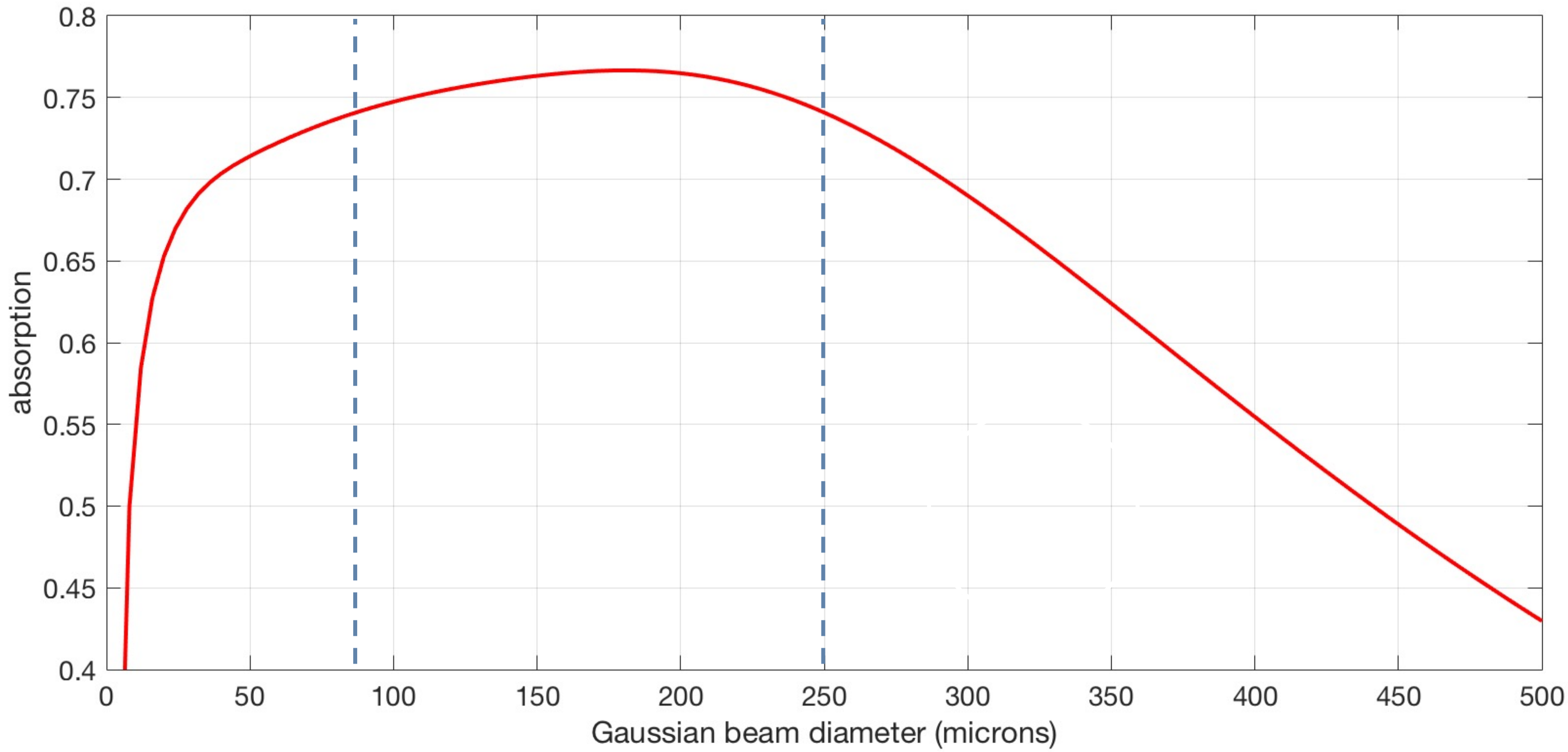

- We can model the efficiency dependence on spot size for TE polarized light
- Optimal spot size is between 90 – 250 µm
- Small spot sizes sample bends and horizontal nanowire regions
- Large spot sizes are vignetted by the edges of the detector

Angular efficiency dependence

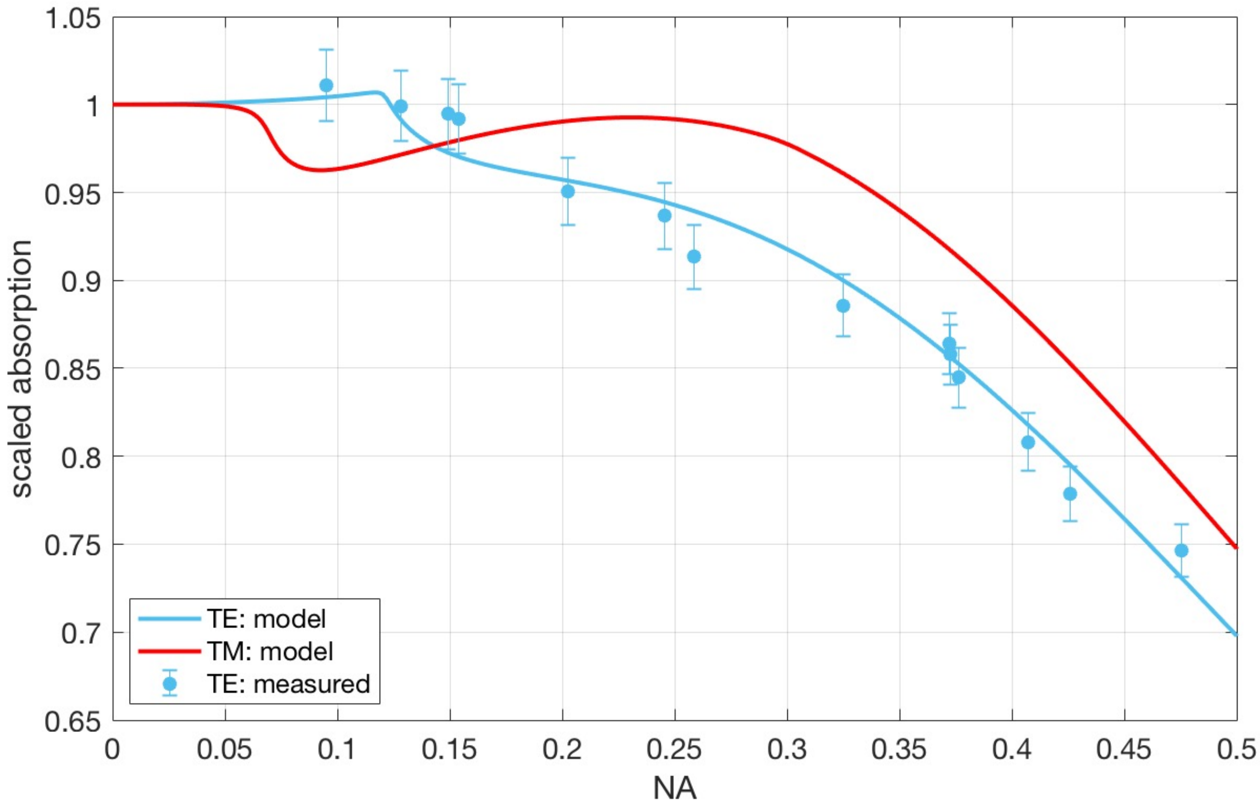

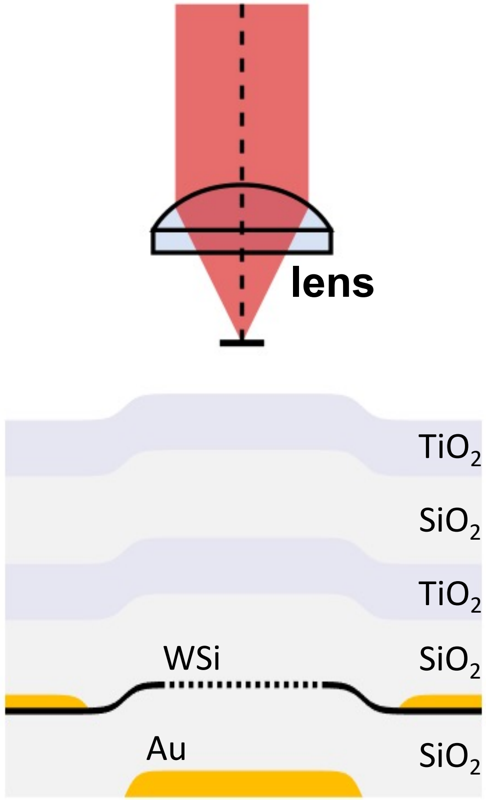

- Limited angular acceptance determines finite numerical aperture of SNSPD
- 10% drop in efficiency at 0.32 NA, >20% drop at 0.42 NA
- Tradeoff in cavity design between collimated beam efficiency and angular acceptance

Dark count rate

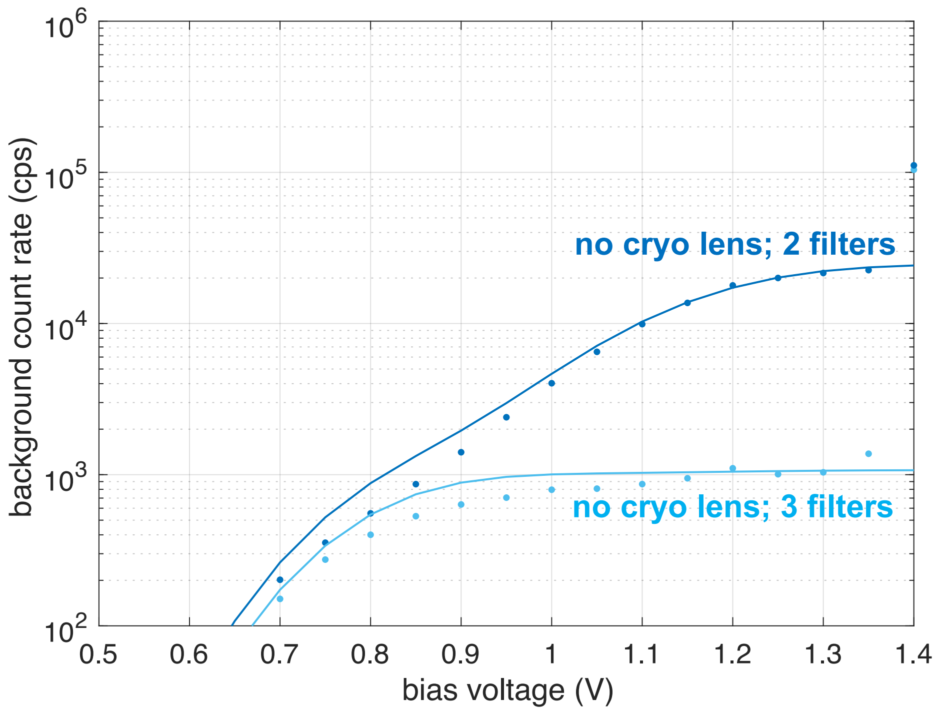

System false count rate with model

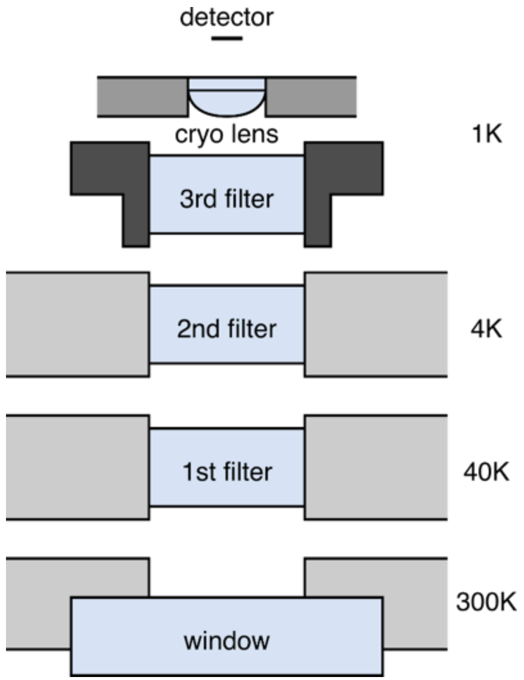

Schematic of cryogenic filter setup

- Dark count rate is dominated by IR blackbody radiation from 300K (DCR w/ 4K window blocked is ~ 1 cps across array)
- Reflective filters on BK7 substrates at 40K and 4K are used to block 300K radiation
- ~1000 cps false count rate across array with lens outside cryostat (16 cps per pixel)
- Expect ~10 kcps across array with increased FOV of cryogenic lens

Dark count rate

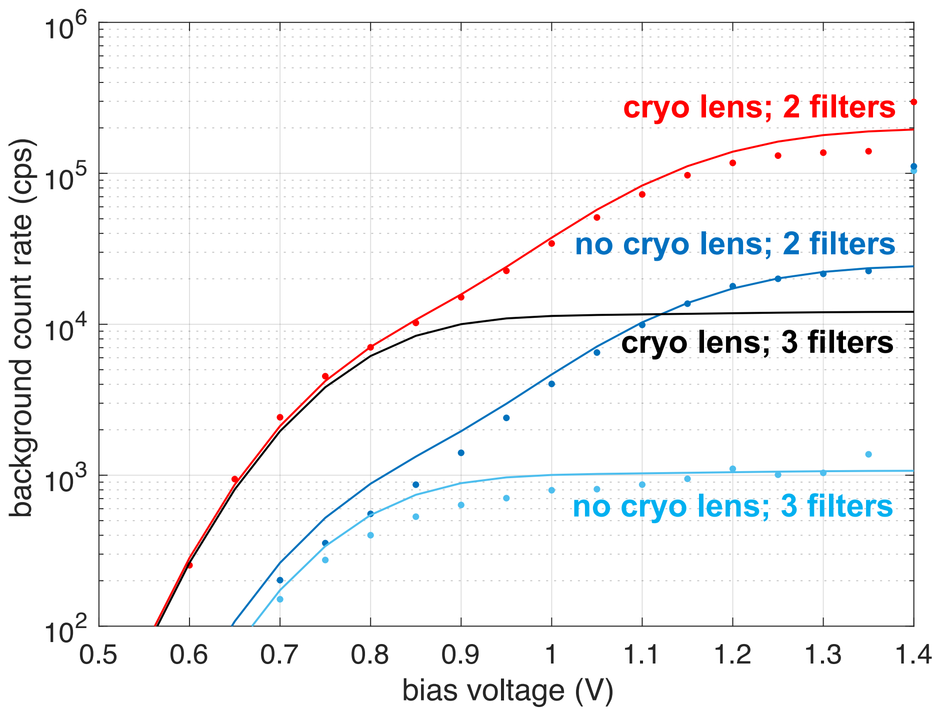

System false count rate with model

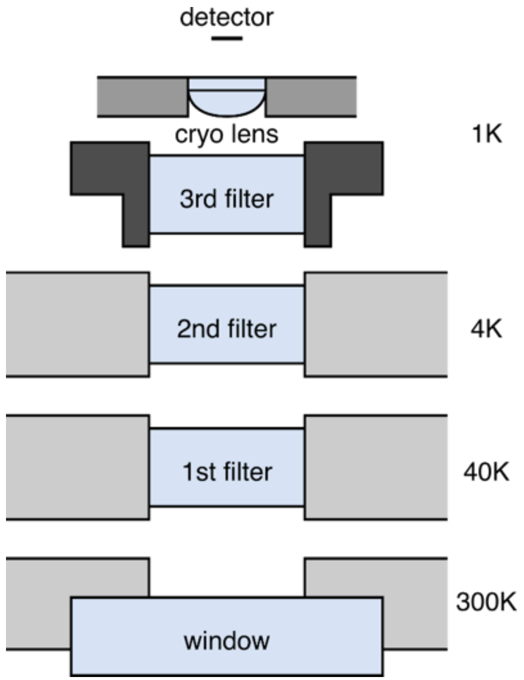

Schematic of cryogenic filter setup

M
D

- Dark count rate is dominated by IR blackbody radiation from 300K (DCR w/ 4K window blocked is ~ 1 cps across array)
- Reflective filters on BK7 substrates at 40K and 4K are used to block 300K radiation
- ~1000 cps false count rate across array with lens outside cryostat (16 cps per pixel)
- Expect ~10 kcps across array with increased FOV of cryogenic lens

Maximum count rate

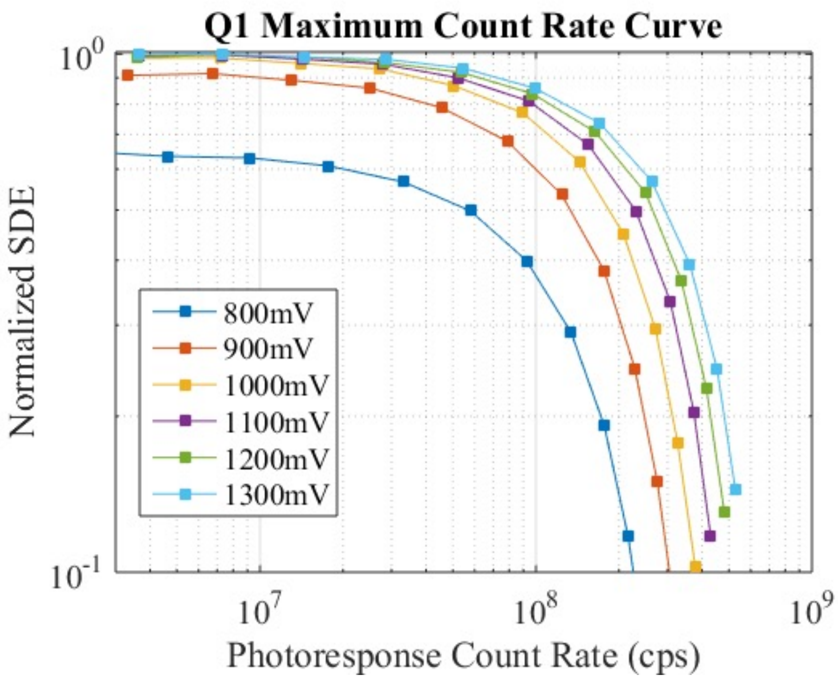

Maximum count rate measured for one 16-channel quadrant

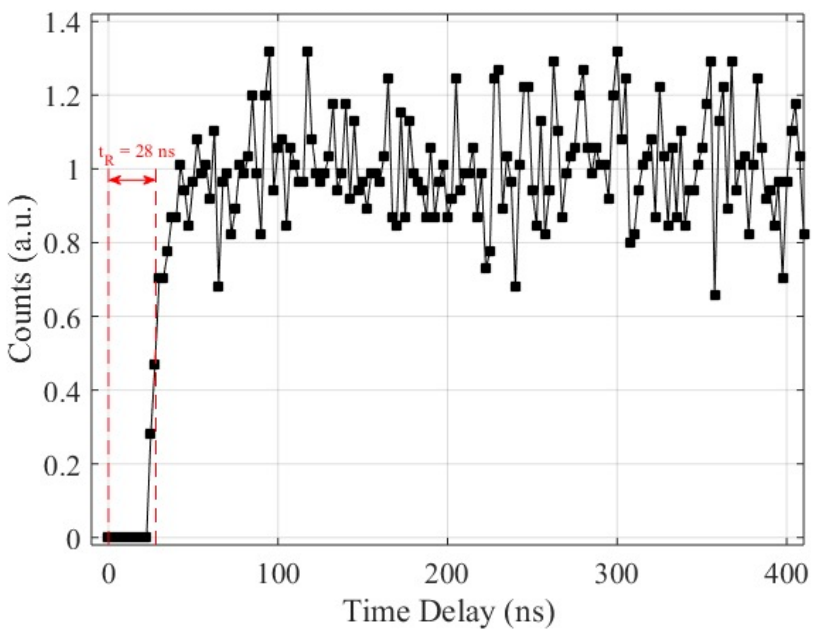

Interarrival time histogram showing 28 ns dead time, no afterpulsing

- MCR measured with beam centered on a single quadrant due to count rate limitations in TDC
- 120 – 300 Mcps 3dB point per quadrant
- Scales to 465 – 1160 Mcps across 62 pixels
- Present total counting rate is limited to 900 Mcps by time tagging electronics

Maximum count rate vs. signaling format

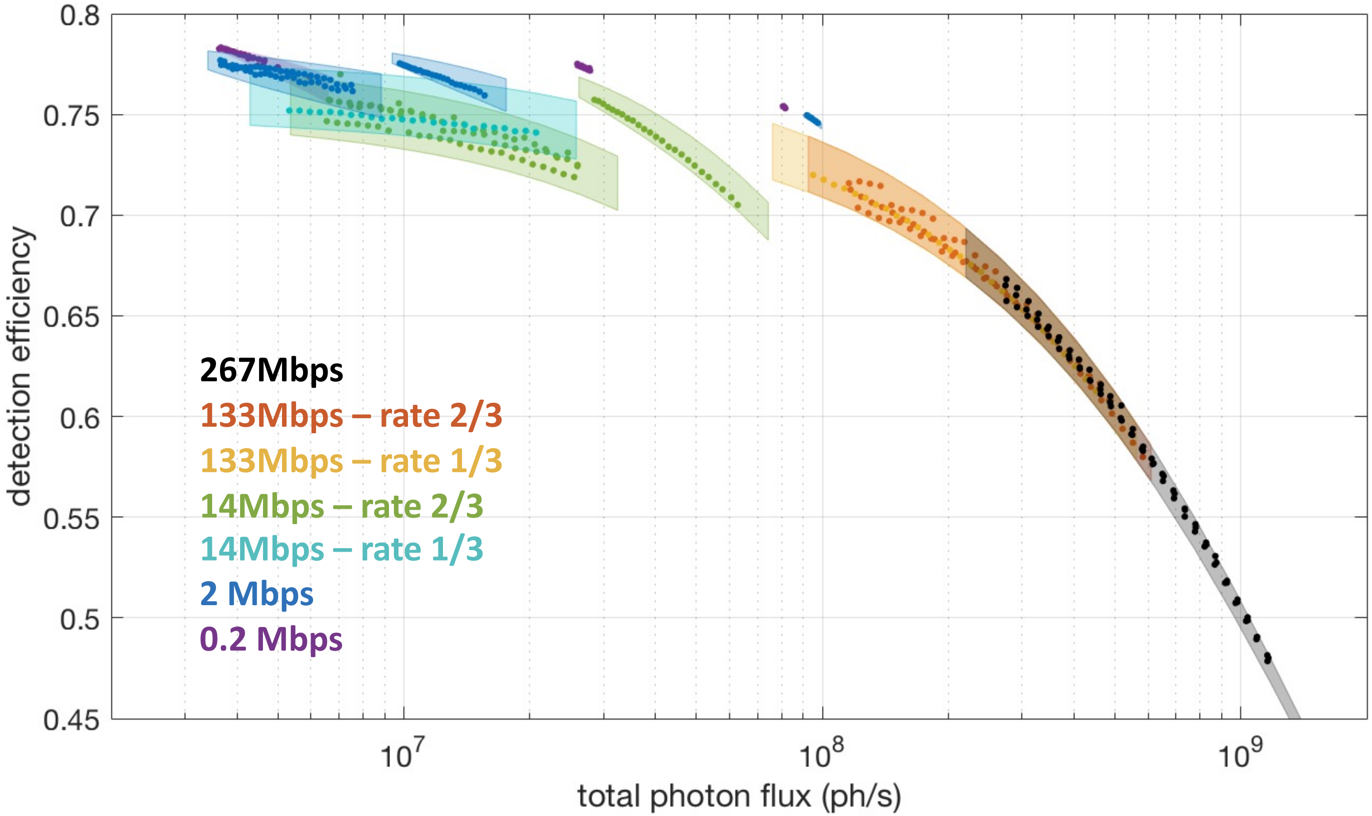

- To fully model the system detection efficiency for a given spot size, NA, signal format, and photon flux, we can combine the optical absorption model, the measurements of blocking loss, and the arrival time statistics of the signal and background photons into a model that calculates the average time between registered events for each channel.
- Comparison of modeled to measured results during end-to-end testing provides high confidence in the model predictions

Timing jitter of SNSPD and TDC

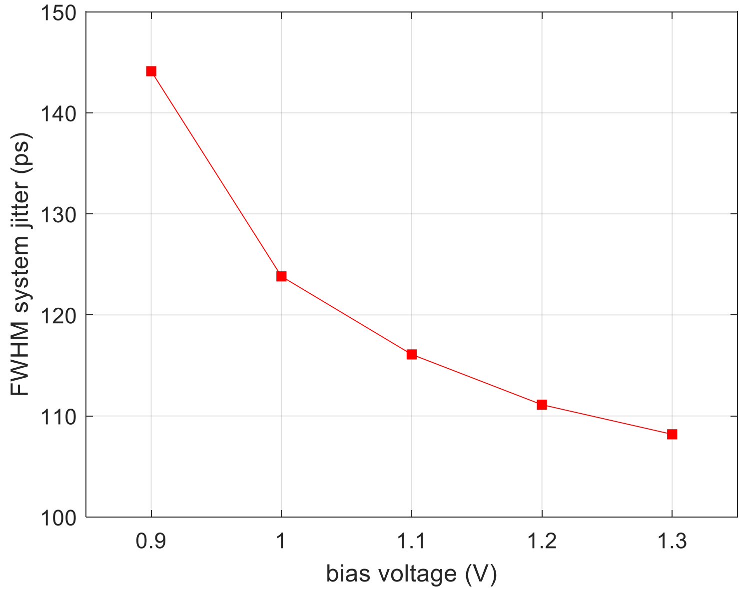

System jitter vs. bias voltage

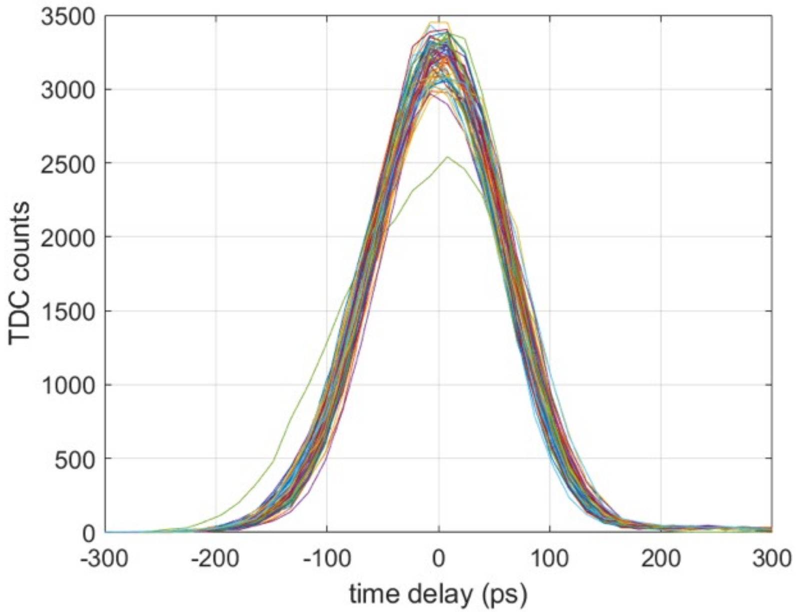

Instrument response function for each pixel, histogram of TDC time tags

- Total system jitter < 120 ps FWHM at low flux rates.
- TDC jitter alone ~ 50 ps

Walk-induced jitter

- At higher count rates, it is more likely that the detector will fire before current has completely returned to the nanowire, producing smaller pulses.
- With a fixed threshold comparator, different pulse heights result in different time delay offsets (walk).
- Without compensation, walk increases overall jitter.

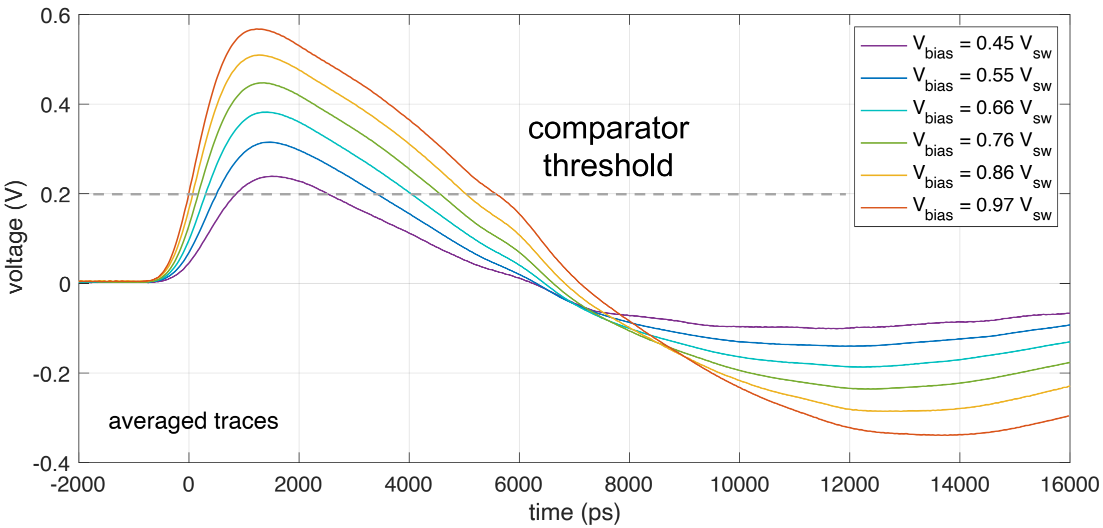

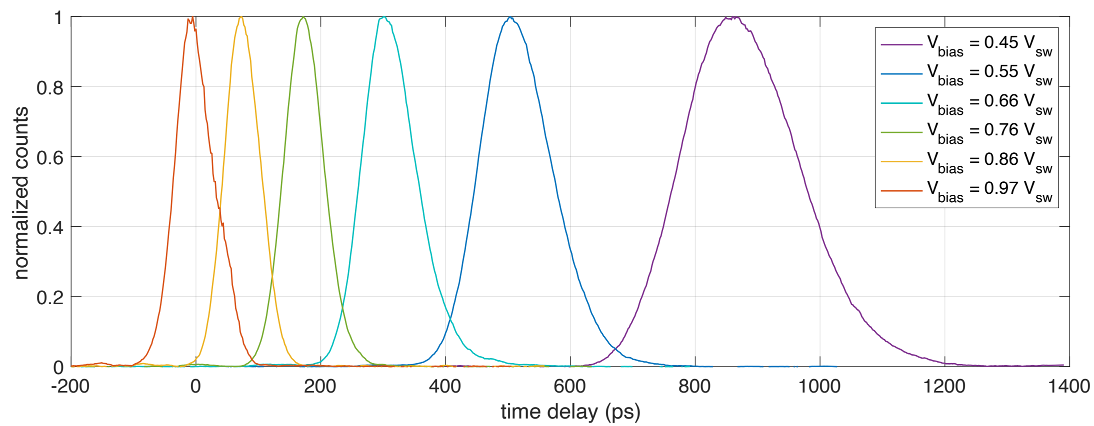

Walk-induced jitter

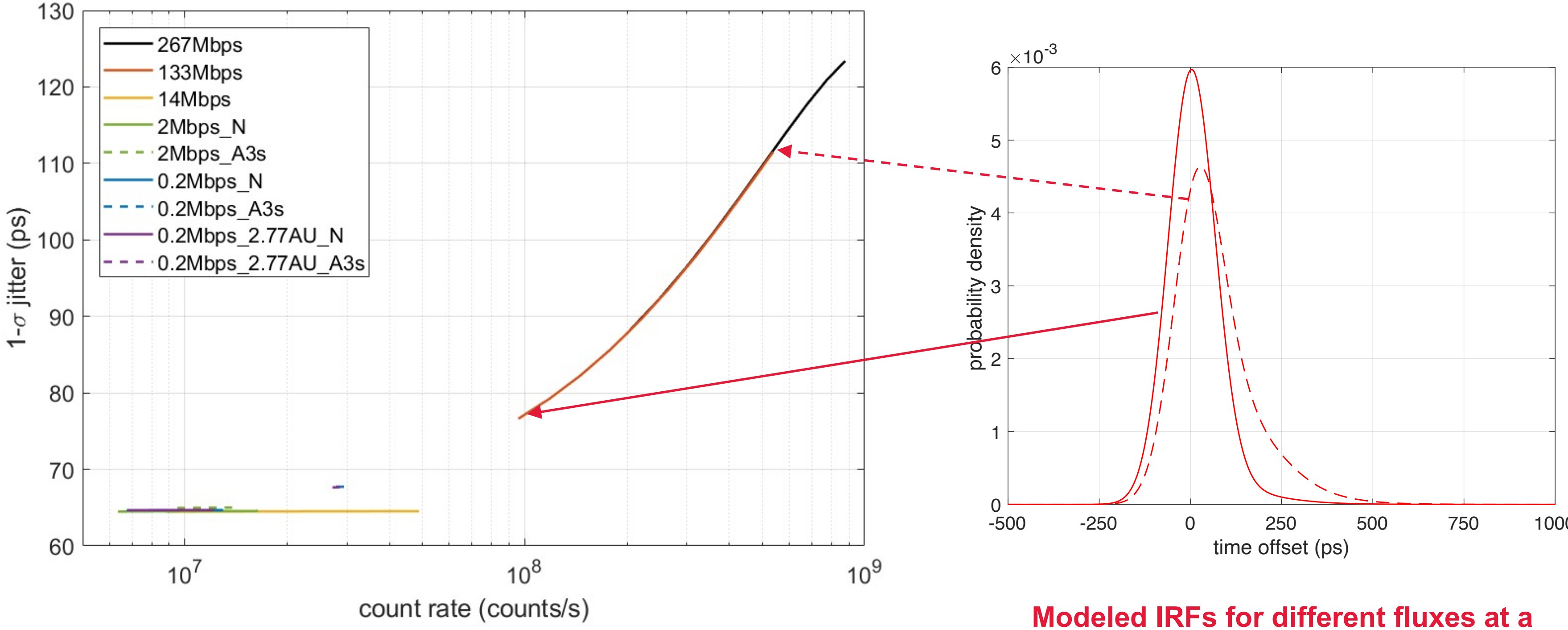

Estimated timing jitter as a function of count rate for different signaling formats

Modeled IRFs for different fluxes at a 133 Mbps data rate

- We can model the distribution of bias currents during photon absorption events for different signaling formats and predict the resulting jitter.
- Even at the highest rates, the system jitter meets our 125 ps requirement.
- For future SNSPD receivers, a constant fraction discriminator should be used to eliminate walk.

End-to-end receiver testing

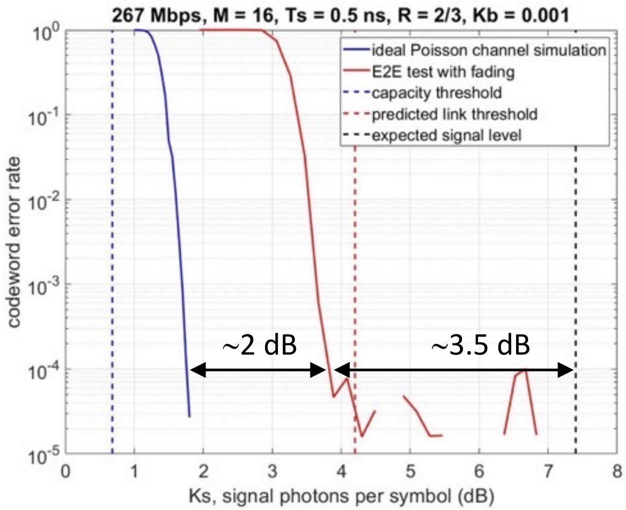

error rate vs. signal out of the detector

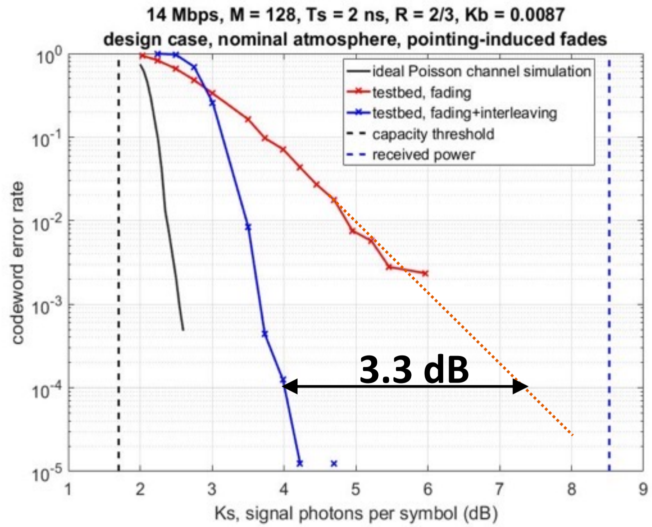

testing interleaving gains

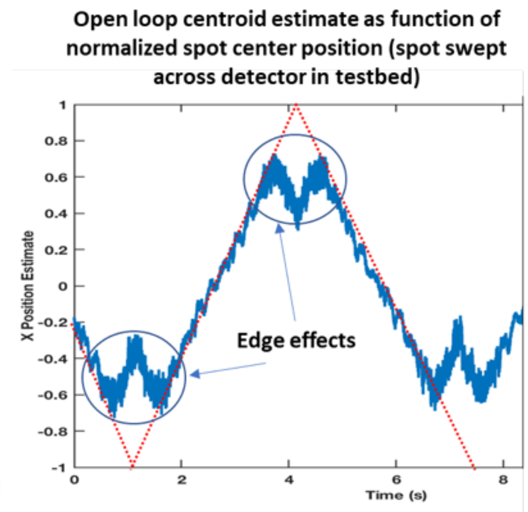

testing centroiding estimates

- To test the performance of the ground receiver system, we can send data with a fiber-coupled modulated laser into the free-space optics.
- Initial round of end-to-end tests **closed links** at data rates from 0.2 Mbps to 267 Mbps under realistic signal and background fluxes.
- Examples of tests:
  - Link budget verification
  - Functionality of interleaver in the presence of fading
  - Error rate as spot is moved off of array
  - Effect of clock drift
  - Slot synchronization

Future challenges for optical communication

- Beyond DSOC, future receivers will require 10x larger active areas, 6x higher count rates
- Example: RF-optical hybrid with mirror panels on existing radio dishes to achieve larger apertures

DSN antenna at Goldstone, CA

Increasing area without sacrificing speed

- Speedup resistors can decrease electrical recovery time in long nanowires to match the thermal relaxation time.
- Some materials (e.g. NbN) have faster thermal relaxation times
- Wider nanowires can cover larger areas with the same pitch and number of squares

MIT

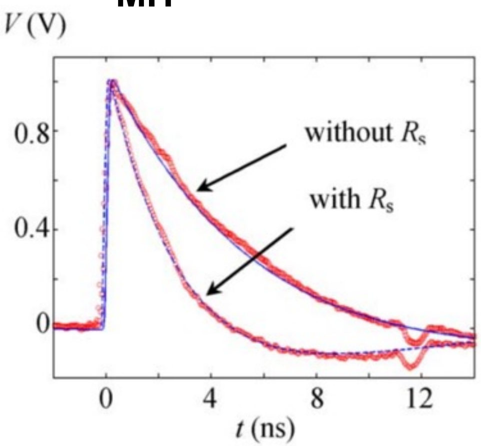

J.K.W. Yang, A.J. Kerman, E.A. Dauler, V. Anant, K.M. Rosfjord, and K.K. Berggren. *IEEE Trans. Appl. Supercond. 2007.*

JPL

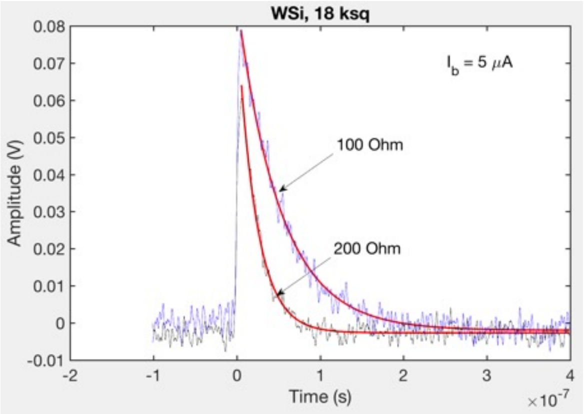

E. Ramirez and B. Korzh

NIST

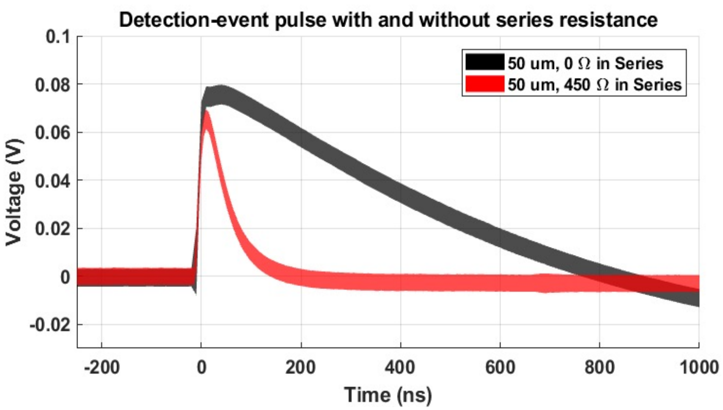

D.V. Reddy, R.R. Nerem, A.E. Lita, S.W. Nam, R.P. Mirin, and V.B. Verma. CLEO 2019

Improving timing resolution: Ultra high time resolution

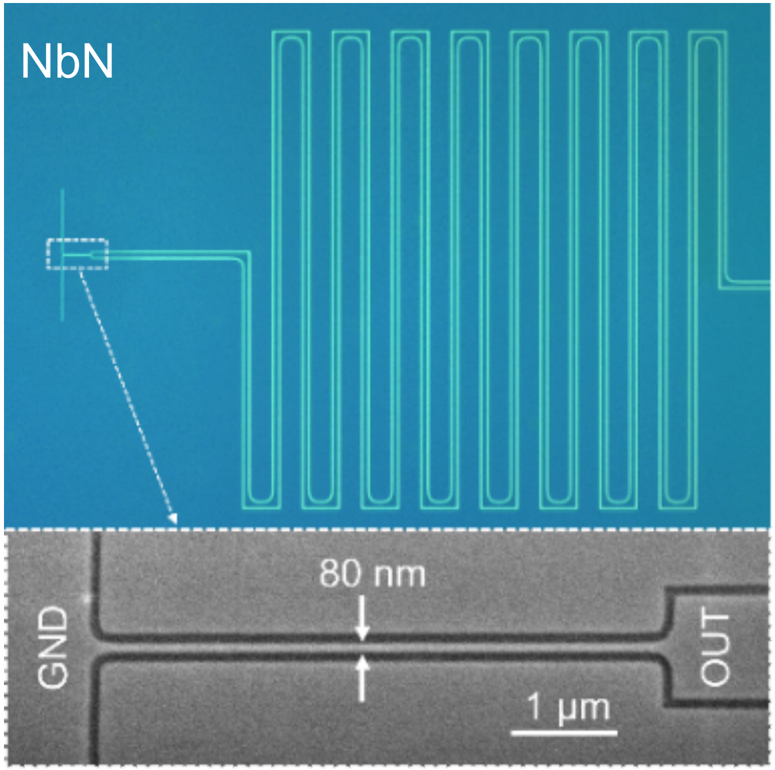

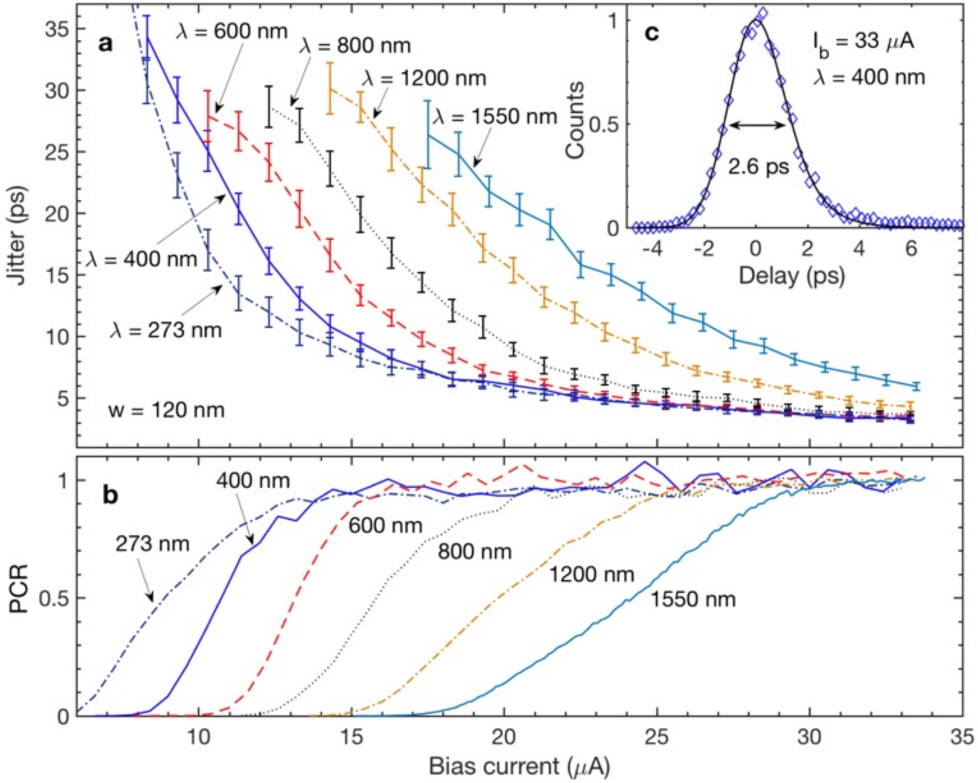

- Short nano-bridge to limit the geometric contribution.
- Study of fundamental limits.

- **Record time resolution for free-running single photon detector: 2.6 ps FWHM**
- Photon energy dependence indicates presence of intrinsic effects due to detection mechanism.

Improving timing resolution: differential readout

- 61% SDE @ 1550 nm;
- 15 ps jitter (300K LNA)

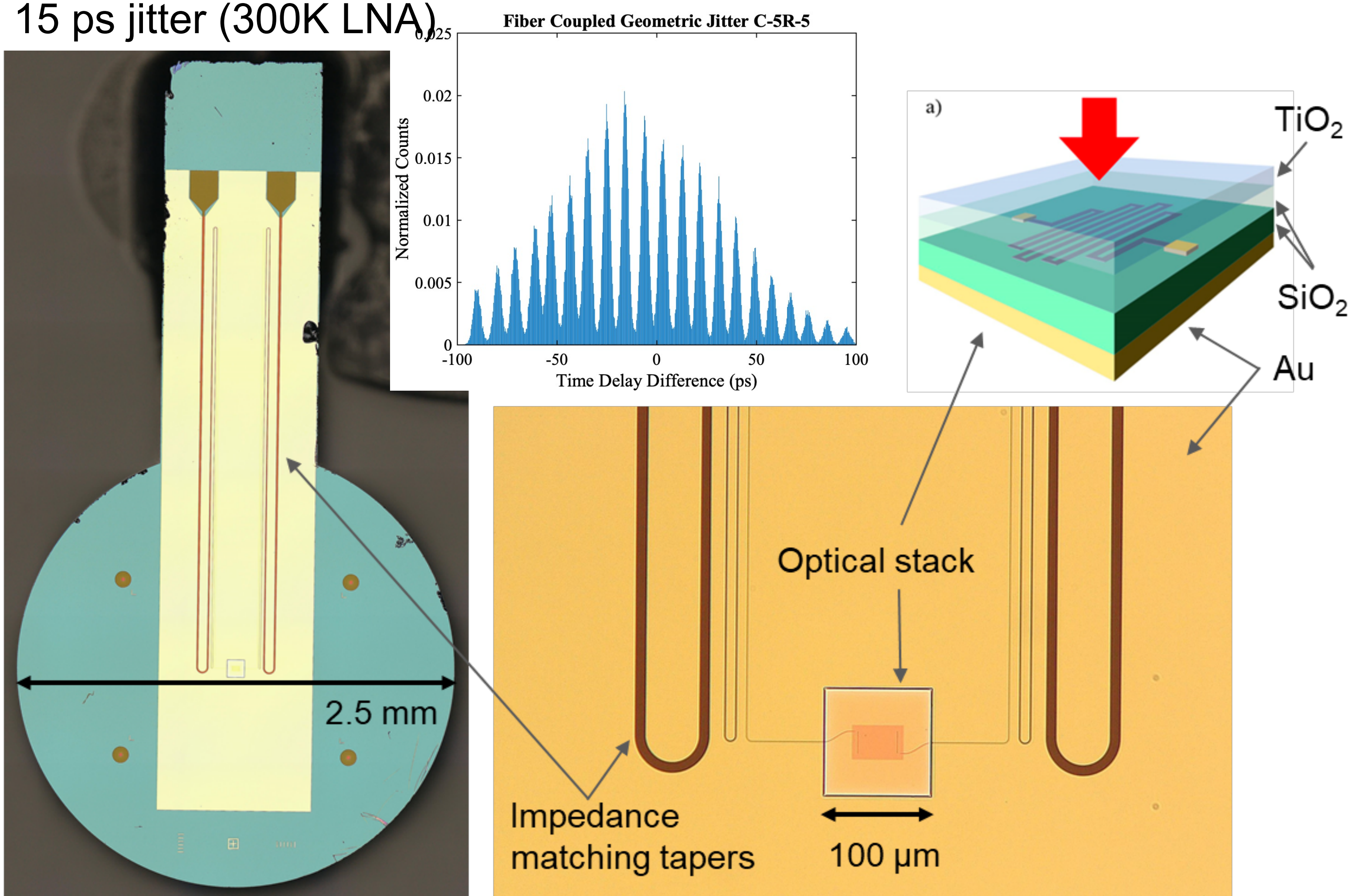

Improving timing resolution: differential readout

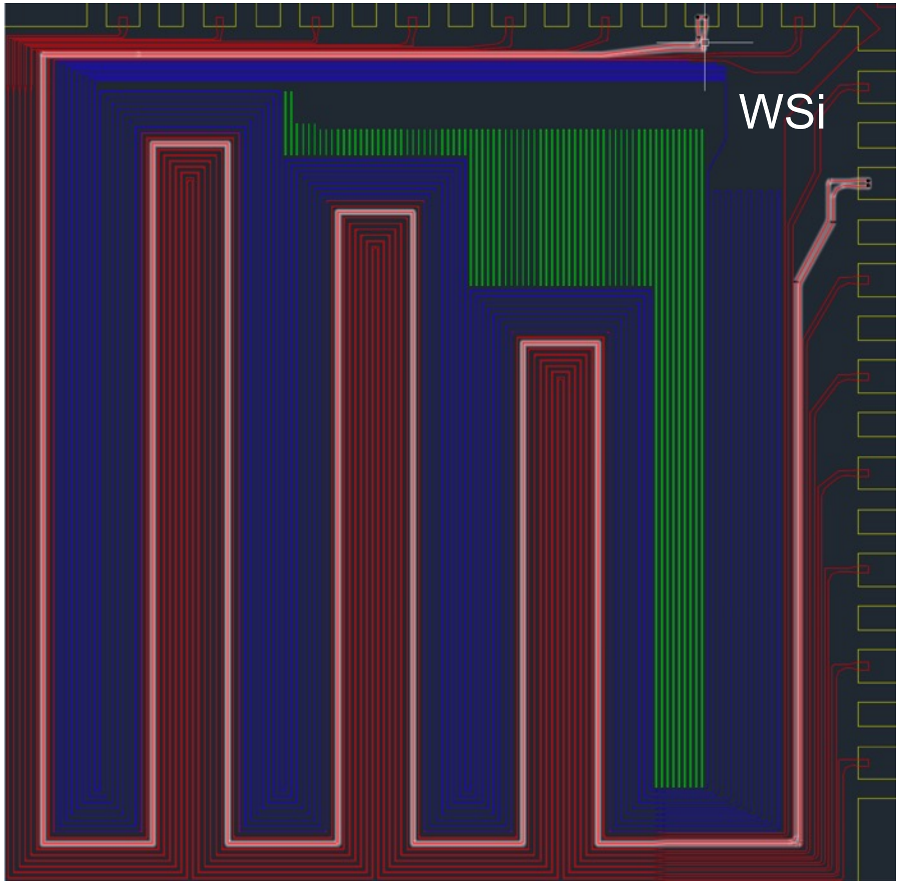

- Differential readout of each nanowire.
- Cancels out the latency changes due to absorption in different nanowire sections.

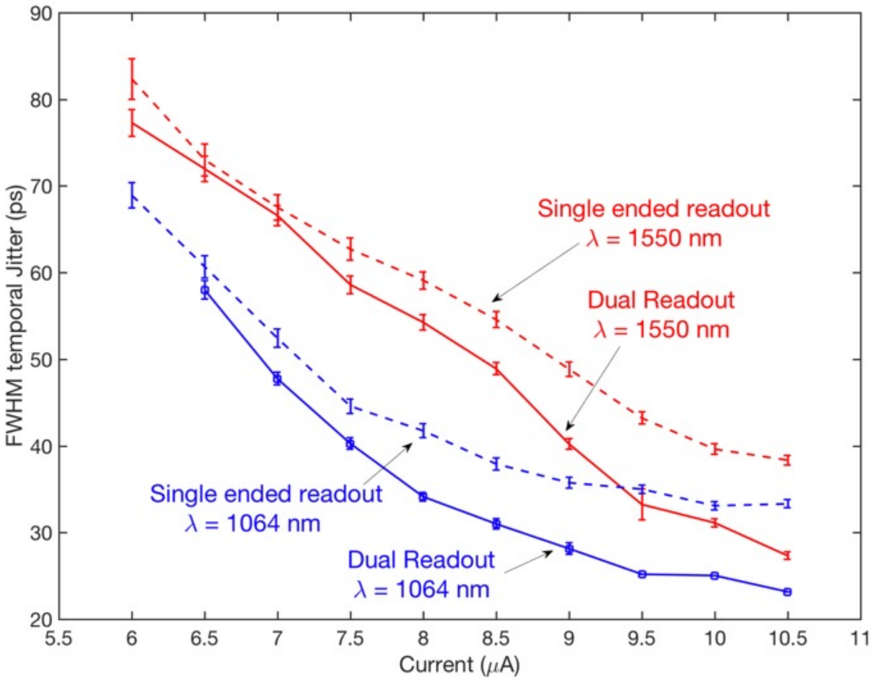

- Jitter reduction due to differential readout scheme compared with single ended readout with the same cryogenic amplifiers.
- Photon energy dependence indicates intrinsic limits are being approached for telecom wavelengths.
- **Jitter reduced to < 30 ps FWHM**

Summary and Future Directions

- Deep space laser communication offers 10-100x higher data rates than Ka-band radio for equivalent mass and power on the spacecraft
- NASA DSOC project will provide the first demonstration of laser comm from beyond lunar orbit, with free-space links up to ~400 million km
  - 64-pixel SNSPD arrays are a key technology for the ground receiver at Palomar observatory
  - Future optical Deep Space Network will require ~10x larger and faster SNSPD arrays

Hale Telescope, Palomar Observatory

Image credit: Palomar Observatory California Institute of Technology

JPL SNSPD development team

JPL Staff


Matt Shaw (389I)


Emma Wollman (389I)


Andrew Beyer (389I)


Ryan Briggs (389R)


Marc Runyan (389I)

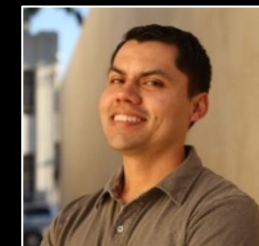
Angel Velasco (337E)

Postdocs


Boris Korzh

Graduate Students


Jason Allmaras


Andrew Mueller


Edward Ramirez

Alumni


Jeff Stern 1962-2013

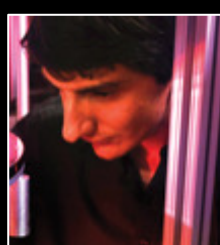
Francesco Marsili


Bill Farr

Collaborators:

NIST

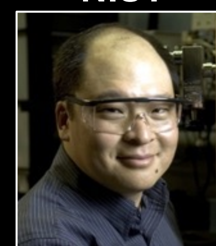
Sae Woo Nam

Caltech


Maria Spiropulu

MIT

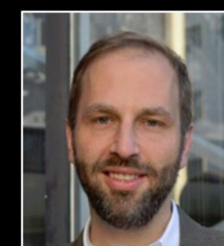
Karl Berggren

Other groups at MIT, UCSD, Caltech, Duke, Sandia, & industry

Jet Propulsion Laboratory
California Institute of Technology

jpl.nasa.gov

Modeled absorption vs. wavelength

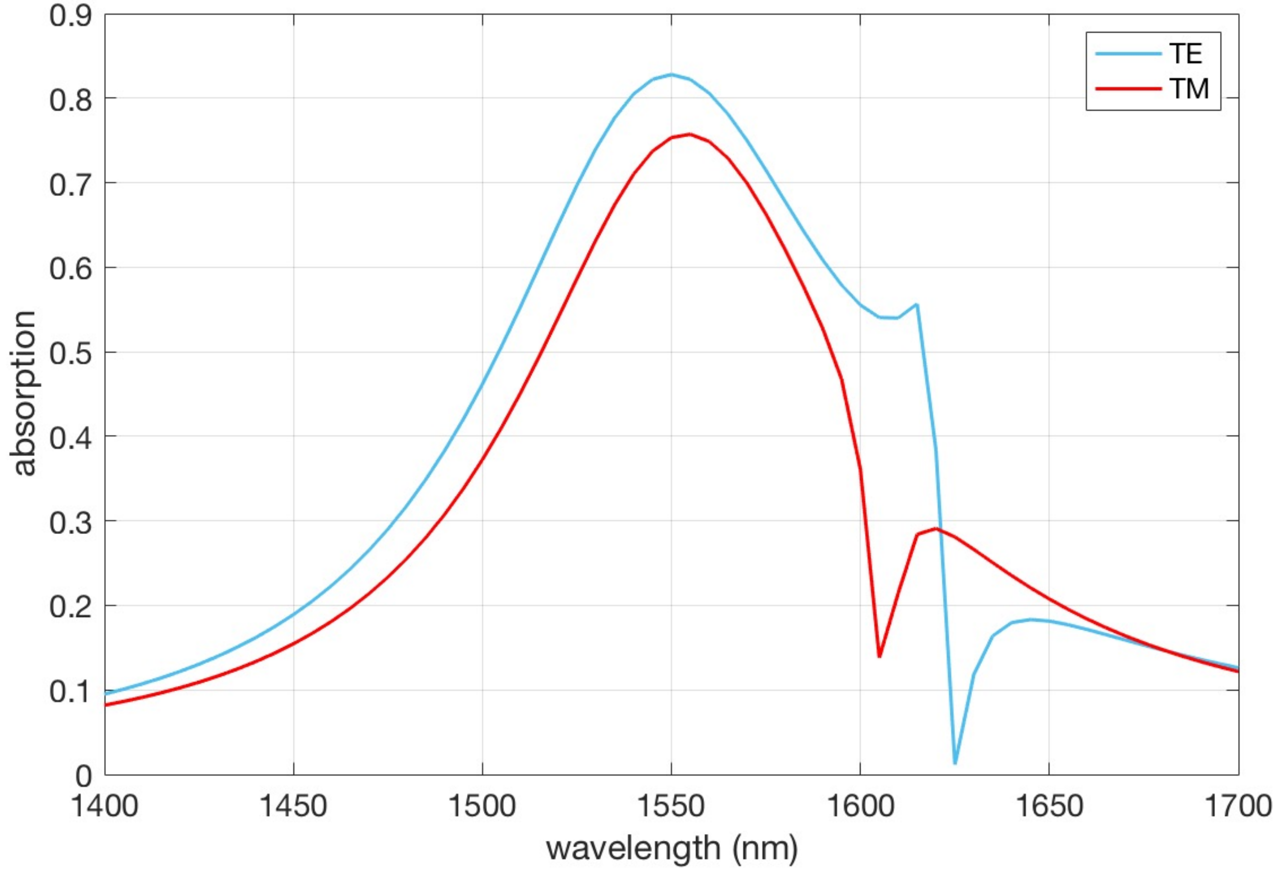

Spatial model: 60 micron and 230 micron spots

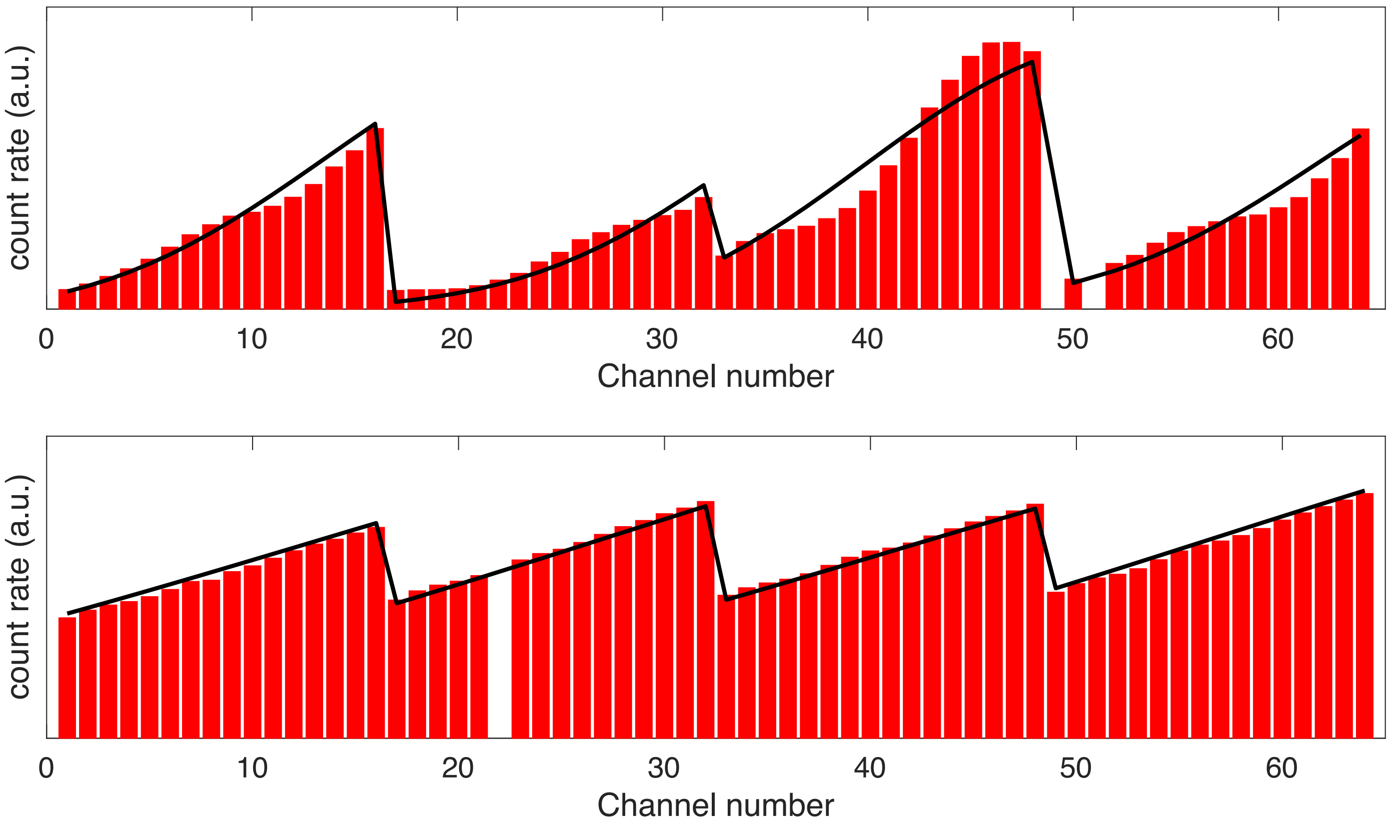

Angular efficiency dependence

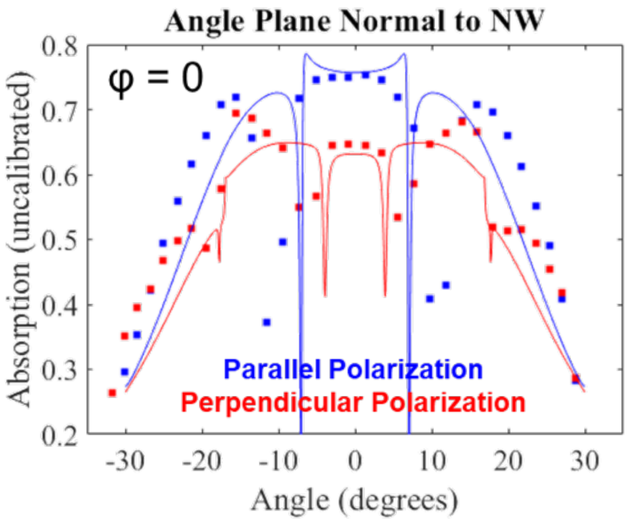

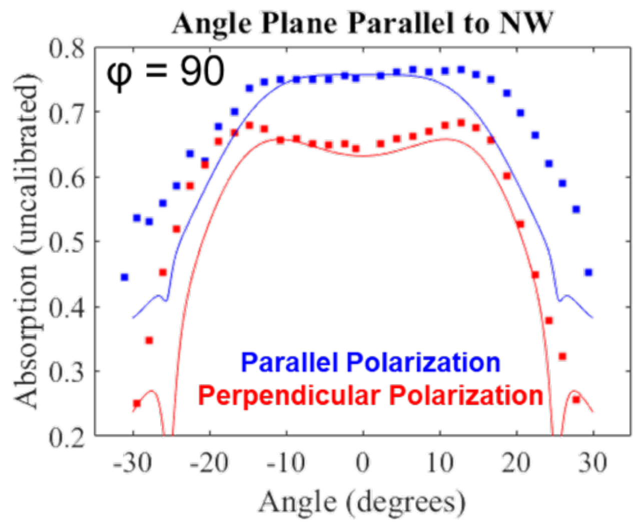

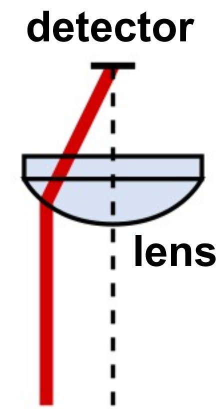

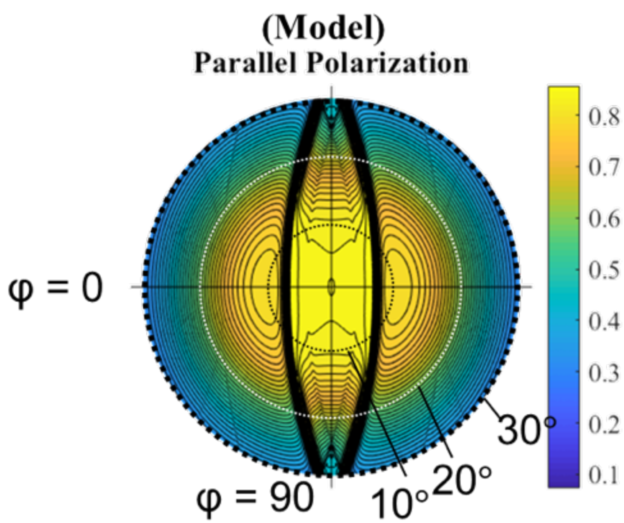

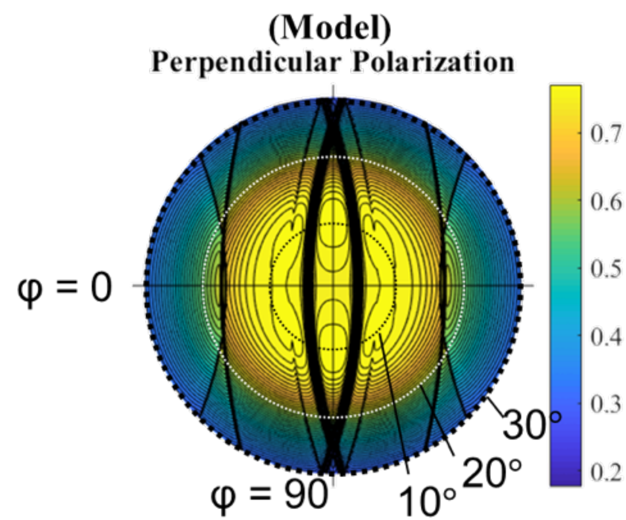

RCWA model and measurements